



Rediscovery of the toadlet *Brachycephalus bufonoides* Miranda-Ribeiro, 1920 (Anura: Brachycephalidae) with osteological and acoustic descriptions

MANUELLA FOLLY^{1,2,3}, LUCAS COUTINHO AMARAL², SERGIO POTSCH DE CARVALHO-E-SILVA² & JOSÉ P. POMBAL JR.¹

¹Universidade Federal do Rio de Janeiro, Departamento de Vertebrados, Museu Nacional, Quinta da Boa Vista, 20940-040 Rio de Janeiro, RJ, Brazil.

²Universidade Federal do Rio de Janeiro, Laboratório de Anfíbios e Répteis, Departamento de Zoologia, Caixa Postal 68044, 21944-970, Rio de Janeiro, RJ, Brazil.

^{1,2,3} follymga@gmail.com; <https://orcid.org/0000-0002-5353-3906>

¹ pombal@acd.ufrj.br; <https://orcid.org/0000-0003-4900-630X>

² lamaral94@gmail.com; <https://orcid.org/0000-0001-5411-5522>

² spotsch@gmail.com; <https://orcid.org/0000-0001-7558-4926>

³Corresponding author

Abstract

Brachycephalus bufonoides was described as a “variety” of *B. ephippium* based on two specimens which 90 years later was considered full species. Besides its brief original description, nothing else is known for this species. Herein we report the rediscovery of the pumpkin-toadlet *Brachycephalus bufonoides* from Nova Friburgo, State of Rio de Janeiro, the second most populous area within the Atlantic Forest in Brazil. A detailed osteological description of this species was also provided, including skull, hyolaryngeal skeleton and postcranium skeleton. The laryngeal skeleton of *Brachycephalus* genus was depicted for the first time. We conducted a molecular phylogenetic analysis of *Brachycephalus* using DNA sequences comprising two fragments of mitochondrial gene (16S). Both analysis with Bayesian inference and maximum parsimony supported the recognition of *B. bufonoides* as an exclusive lineage, allocated within the *B. ephippium* species group in *B. vertebralis* lineage. We improved the diagnosis and variation of the species, including more collected specimens, coloration *in vivo* and advertisement call description. Compared with its congeners, *B. bufonoides* has skin on head and dorsum with dermal hyperossification; skull with hyperossification of postorbital crests; a pair of hyperossified bulges about equidistant between postorbital crests; fourth presacral vertebra with transverse process hyperossified, ornamented and sacral diapophyses hyperossified, which can be seen externally (lineage of *B. vertebralis sensu* Condez *et al.* 2020); presence of dermal ossification as separated bulges of each vertebrae; general background color orange with different intensities of dark orange blotches on dorsum, including bordering of sacral region; absence of osteoderms and presence of warts on the dorsolateral surface of body; medium body size (SVL of adults: 12.0–14.5 mm for males and 14.7–16.3 mm for females; Table 1); rough dorsum; advertisement calls with 13 to 17 pulses; presence of pulse period modulation; and advertisement calls with notes longer than 0.2 s (0.22 to 0.31 s). Herein an important contribution for the taxonomy and systematics of this genus is provided, including a large amount of novel information for *B. bufonoides* from different sources (*i.e.*, molecular, morphological variation, bioacoustic), allowing it to be included in future studies of species delimitation and relationships within *Brachycephalus*. Also, the discovery of this species reiterates the importance of Nova Friburgo for the conservation of the Atlantic Forest biodiversity.

Key words: Atlantic Forest; Brachycephaloidea; Morphology; Natural History; Taxonomy

Introduction

The neotropical anuran family Brachycephalidae Günther, 1858 includes two genera: *Brachycephalus* Fitzinger, 1826 and *Ischnocnema* Reinhardt and Lütken, 1862. *Brachycephalus* is endemic to the Brazilian Atlantic Forest with 36 species (Frost 2019), 21 being described only in the last ten years, which highlights the lack of knowledge about the genus diversity (see Pombal 2010; Bornschein *et al.* 2016; Monteiro *et al.* 2018a). The species show a strong degree of endemism, with 14, of the 21 described the last ten years, are known only from their type locality (Bornschein *et al.* 2019a).

Frogs of the genus *Brachycephalus* live amongst the leaf litter of high-humidity montane forests (Pombal *et al.* 1994; Pie *et al.* 2013), and breed through direct-development, which means that they do not undergo larval phase, thus small toadlets hatch from eggs laid on the forest floor (Pombal *et al.* 1994; Pombal 1999). Little is known about the life history and ecology of *Brachycephalus* species, and most data are limited to their descriptions (but see Pombal *et al.* 1994; Almeida-Santos *et al.* 2011; Dorigo *et al.* 2012; Siqueira *et al.* 2014; Oliveira and Haddad, 2015). Furthermore, of the 36 described species, only 13 have their advertisement call described: *B. actaeus* (Monteiro *et al.* 2018a), *B. albolineatus* (Bornschein *et al.* 2017), *B. crispus* (Condez *et al.* 2014), *B. darkside* (Guimarães *et al.* 2017), *B. ephippium* (Pombal *et al.* 1994), *B. hermogenesi* (Verdade *et al.* 2008), *B. mirissimus* (Pie *et al.* 2018), *B. olivaceus* (Monteiro *et al.* 2018b), *B. pernix* (Wistuba 1998), *B. pitanga* (Araújo *et al.* 2012), *B. quiririensis* (Monteiro *et al.* 2018b), *B. sulfuratus* (Condez *et al.* 2016), and *B. tridactylus* (Garey *et al.* 2012; Bornschein *et al.* 2019b).

Species of *Brachycephalus* generally have a SVL of 7.4 to 18.9 mm (see Pombal and Izecksohn 2011; Condez *et al.* 2016), absence of sternum; usually eight presacral vertebrae; palatal shelf of maxilla lacking pterygoid process; neopalatines slender (absent in *B. crispus*, *B. ephippium*, *B. ferruginus*, *B. guarani*, *B. hermogenesi*, *B. pernix*, *B. pombali*, and *B. sulfuratus*; see Hedges *et al.* 2008; Clemente-Carvalho *et al.* 2011; Condez *et al.* 2014; Condez *et al.* 2016); columella absent; fenestra ovalis directed posteriorly; arrow-shaped terminal phalanges; one phalange in Finger IV, no phalange or one short phalange in Toe I; terminal digits not expanded; circumferential grooves absent (Hedges *et al.* 2008; Pombal and Izecksohn 2011).

The first molecular hypothesis (Clemente-Carvalho *et al.* 2011) based on 14 *Brachycephalus* species indicated the existence of three species groups. Based on this topology, Ribeiro *et al.* (2015) named such groups based on their congruence with morphological characters (Clemente-Carvalho *et al.* 2011; Ribeiro *et al.* 2015). Subsequently described species were assigned to one of these three groups in their original publication (*e.g.*, Ribeiro *et al.* 2015; Pie and Ribeiro 2015; Bornschein *et al.* 2016). Ribeiro *et al.* (2015) tentatively assigned the remaining species into these previously proposed species groups based on general morphological similarities. *Brachycephalus ephippium* species group is characterized by its dermal ossification, which varies in degree, and is comprised of 12 species: *B. alipioi* Pombal and Gasparini, 2006; *B. bufonoides* Miranda-Ribeiro, 1920; *B. crispus* Condez, Clemente-Carvalho, Haddad and Reis, 2014; *B. darkside* Guimarães, Luz, Rocha and Feio, 2017; *B. ephippium* (Spix, 1824); *B. garbeanus* Miranda-Ribeiro, 1920; *B. guarani* Clemente-Carvalho, Giarretta, Condez, Haddad and Reis, 2012; *B. margaritatus* Pombal and Izecksohn, 2011; *B. nodoterga* Miranda-Ribeiro, 1920; *B. pitanga* Alves, Sawaya, Reis and Haddad, 2009; *B. toby* Haddad, Alves, Clemente-Carvalho and Reis, 2010; and *B. vertebralis* Pombal, 2001. Recently, Condez *et al.* (2020) propose two lineages within *B. ephippium* group, which might be considered further as the *B. vertebralis* lineage (without a bone shield; *Brachycephalus alipioi*, *B. crispus*, *B. guarani*, *B. nodoterga*, *B. pitanga*, *B. toby*, *B. vertebralis*, *B. sp. 2* and *B. sp. 3*) and the *B. ephippium* lineage (exhibiting a bone shield; *B. ephippium*, *B. garbeanus*, *B. margaritatus*, *B. sp. 4*, *B. sp. 5* and *B. sp. 6*).

Brachycephalus bufonoides was described as a “variety” of *B. ephippium* based on two specimens from Serra de Macaé, municipality of Nova Friburgo, State of Rio de Janeiro, Brazil (Miranda-Ribeiro 1920; Bokermann 1966). Later, Cochran (1955) synonymized all varieties of *B. ephippium* (Spix, 1824) (*B. var. nodoterga*; *B. var. garbeanus* and *B. var. bufonoides*) described by Miranda-Ribeiro (1920), including *B. bufonoides*. Heyer *et al.* (1990) revalidated and considered *B. nodoterga* as a full species, while the other varieties were re-evaluated only in Pombal (2010), when *B. bufonoides* was revalidated and considered a full species. The original specimens of *B. bufonoides* were founded by the renowned collector of the Museu Paulista, Ernest Garbe (1853-1925) in 1909, and no other specimens had been found so far, despite the type locality being inserted in the metropolitan region of Rio de Janeiro.

Recently, we collected new specimens from municipality of Nova Friburgo, state of Rio de Janeiro, that match the original description and original specimens of *B. bufonoides*, represented originally by two specimens. By comparing internal and external morphology with the other congeners, we present a redescription for *B. bufonoides* based on these recently collected specimens and provide new osteological, acoustical and molecular information for this species.

Material and Methods

Morphological Assessment

For morphometrics, a single person (M. Folly) took 19 measurements with an ocular micrometer in a Leica MZ-6 stereomicroscope (0.001 mm). All measurements were in millimeters: snout–vent length (SVL; ventral distance from the tip of the snout to cloaca); axilla–groin length (AGL; distance between the axilla and the ending of maxilla); head length (HL; dorsal distance from the tip of the snout to angle of jaw); head width (HW; greatest width of head located between angles of jaw); nostril diameter (ND; maximum width of the nostril); internostril distance (IND; between inner margins of nostrils); nostril–tip of snout distance (NSD; interval between anterior corner of the nostril to the tip of the snout); interorbital distance (IOD; interval between the inner edge of the orbits); eye diameter (ED; width of the eye); eyelid width (EW); eye–nostril distance (END; from anterior corner of the eye to posterior margin of nostril); arm length (AL; distance between axilla to elbow); forearm length (FAL; distance between the elbow to the insertion of the hand); hand length (HAL; between the insertion of the hand and the longest toe); Finger-III length (FIL; insertion between Fingers II-III to the top of Finger III); thigh length (THL; distance from the cloaca to the knee); shank length (SL; distance from the ankle to the knee); foot length (FL; distance between the ankle of the longest toe); and Toe-III length (TL; insertion between Toes II-III to the tip of Toe III). Except for FL, which is modified to include tarsus length; all of these measurements follow Duellman (1970), Cei (1980), and Heyer *et al.* (1990). Some measurements (ND, NSD, ED, FIL and TL) were also included because they are informative and currently adopted by taxonomists working with this group of species. Nineteen collected specimens were determined as adult males and females by examination of gonads and/or secondary sexual characters. We used the museum acronym of Sabaj (2016). Additional specimens examined are presented in Appendix I.

Three specimens (ZUFJR 15430, 15535, 15536) were cleared and double-stained for osteological observations, following the methods of Taylor and Van Dyke (1985), with few modifications, for osteological observations. One specimen was stained (MNRJ 91688) searching for osteoderms on the skin. The lectotype of *Brachycephalus bufonoides* (MZUSP 1459) was scanned on a Skyscan 1176 in-vivo high-resolution micro-CT scan at Universidade de São Paulo, Brazil. The specimen was scanned at 45 kV and 550 μ A, and the dataset was rendered in three dimensions using CTvox for Windows 64 bits version 2.6.

Terminology of cranial osteology follows Pugener and Maglia (1997), Campos *et al.* (2010) and Trueb (2015); terminology of hyolaryngeal skeleton follows Trewavas (1933), that of pectoral girdle follow Trueb (1973), manus and pes follow Fabrezi (1992; 1993; 2001), and that of vertebral column follow Campos *et al.* (2010). Drawings were made using a stereomicroscope equipped with a camera lucida (Leica MZ-6).

Acoustical Assessment

Vocalizations were recorded with a Tascam DR-07 digital recorder, coupled with a Sennheiser ME-67 shotgun microphone, at a sampling rate of 44.1 kHz and sample size of 16 bits. The species were recorded at Área de Proteção Ambiental (APA) de Macaé de Cima, municipality of Nova Friburgo on 3 October 2015. Air temperature was measured at the time of recording with a portable digital thermo-hygrometer (Minipa MT-242). We analysed three calls from three different males recorded during fieldwork with one voucher specimen (ZUFJR 15424). For acoustic analysis, we used the software Raven Pro 1.4 (Cornell Laboratory of Ornithology Bioacoustics Research Program), with temporal parameters measured directly from the oscillogram, and spectral parameters from the spectrogram (using the Hanning window function, amplitude logarithmic, a window size of 512 samples, and overlap 99%). The graphs were exported using the Raven Pro 1.4 tool for the oscillogram and audiospectrogram, and the R package (R Core Team 2016) Zoo (Zeileis and Grothendieck 2005) for the scatterplot.

Call parameters are divided in temporal and spectral parameters, the definitions and terminologies follow Littlejohn (2001) and Köhler *et al.* (2017) and were analysed using the note-centered approach (*sensu* Köhler *et al.* 2017; see Hepp and Pombal 2019). Temporal parameters: call duration, in minutes (measured in the field with a digital timer, and from the beginning of the first pulse of the first note to the end of the last pulse of the last note in the recordings); note duration, in millisecond (ms) (from the beginning of the first pulse to the end of the last pulse of the same note); note period, in ms (from the beginning of the first pulse of a note till the beginning of the first pulse of the following note); inter-note interval, in ms (from the end of the last pulse of one note till the beginning of the first pulse of the following note); note repetition rate, in note/second (total number of notes divided by the duration

from the first note to the beginning of the last note of the call); number of pulses per note (total number of pulses emitted as a sequence in a note); pulse period, in ms (from the beginning of a pulse of a note till the beginning of the consecutive pulse of the same note); pulse repetition rate, in pulses/second (total number of pulses in a given note divided by the duration from the beginning of the note till the beginning of its last pulse). Spectral parameters: amplitude, in dB; dominant frequency (most energetic frequency band in a given note); minimum frequency (lowest frequency in fundamental bandwidth); maximum frequency (highest frequency in bandwidth). Temporal parameters were measured from the oscillogram and obtained automatically with Raven, fundamental frequency was measured from the spectrogram obtained from the Raven automatic analysis, and are given in numerical range, mean value (\bar{x}), standard deviation (\pm), median (\tilde{x}), and mode (Mo). Some definitions and parameters were referred to as other terms by other authors, and this divergence is specified and discussed below.

Sound recordings were deposited in the acoustic collection of the Setor de Herpetologia, Departamento de Vertebrados, Museu Nacional, Universidade Federal do Rio de Janeiro, Brazil (MNVOC 063).

Molecular Assessment

We obtained tissue samples from five individuals (ZUF RJ 15424, 15425, 15426, 15428, 15429) of *Brachycephalus bufonoides* (Appendix II). The liver samples were preserved in absolute ethanol. We extracted DNA using a DNeasy extraction kit (Qiagen, Valencia, CA, USA). We sequenced 16S ribosomal RNA with adjacent tRNA-Val (999 bp) due to the availability of sequences of this gene in GenBank for other species of *Brachycephalus*, previously studied by Clemente-Carvalho *et al.* (2011), Padial *et al.* (2014), Condez *et al.* (2016), Firkowski *et al.* (2016), and Monteiro *et al.* (2018a). Specimens used in molecular analyses and GenBank accession numbers are in the Appendix II. We performed polymerase chain reactions (PCR) using PCR Master Mix and a pair of primers for each fragment: 16SL2A forward (CCAAACGAGCCTAGTGATAGCTGGTT) and 16SH10 reverse (TGATTACGCTACCTTTG-CACGGT), previously published in Hedges (1994); and, 16Sar forward (CGCCTGTTTATCAAAAACAT) and Wilkinson2 reverse (GACCTGGATTACTCCGGTCTGA), previously published in Palumbi *et al.* (1991) and Wilkinson *et al.* (1996). Thermocycling for DNA amplification for the first fragment began with a denaturation at 95 °C (3 min), followed by 35 cycles of denaturation at 95 °C (30 sec), annealing at 48–50 °C (45 sec), extension at 72 °C (1 min), and a final step at 72 °C following the final cycle (5 min). PCR products were visualized in 1% agarose gels and sent to Macrogen Inc., Seoul, South Korea for purification and sequencing reactions.

Chromatographs were checked manually, assembled, and edited using Geneious 8.1.7 (Kearse *et al.* 2012), adjusted manually to generate consensus sequences for each specimen. Sequences were checked with Basic Local Alignment Search Tool (BLAST; Altschul *et al.* 1997) against the GenBank nucleotide database to ensure that the amplified product was correct and not contaminated. Both 16S fragments were concatenated for phylogenetic reconstruction. We aligned and compared each fragment (both 16S partitions) for each individual and removed parts of the fragments that exhibited any degree of overlap. We aligned sequences using MAFFT v7.130b (Kato and Standley 2013), with a gap opening penalty of 1.53 and an offset value of 0.0, parameter was set to the G-INS-i model. Models of molecular evolution for use in Bayesian analyses were estimated using the Akaike information criterion (AIC) in jModeltest 2.17 (Posada 2008), the model chosen was GTR+G.

We used the mitochondrial 16S rRNA fragment to calculate the genetic distances (maximum intraspecific and minimum interspecific) among the species of *Brachycephalus*. We estimated the uncorrected pairwise distances using MEGA 6 (Koichiro *et al.* 2013), with pairwise deletion of missing information.

Phylogenetic trees were obtained using Bayesian inference (BI) and maximum parsimony (MP) analyses. BI was performed with MrBayes v. 3.2 (Ronquist *et al.* 2012) with four independent runs, each one with four MCMC chains running for 10,000,000 generations, with a sampling frequency of 2000. Convergence of sampled parameters was checked in Tracer 1.5 (Rambaut and Drummond 2007), and the first 15% of sampled trees and parameters were discarded as burn-in. Branch support was assessed by posterior probability. MP analysis was conducted using tree new technology (TNT) v1.5 (Goloboff *et al.* 2003). The shortest trees (i.e., most parsimonious trees) were reached through heuristic search (= traditional search) with 10000 random addition sequences, random seed = 0 (i.e., according to time when the analysis was conducted), tree bisection–reconnection algorithm, and holding 100 trees per replicate. A second search (same parameters) was conducted with the trees held in the memory of TNT. The trees were allowed to be collapsed afterward, with collapse rule = 3 (collapse branch if some optimization lacks support).

The strict consensus tree was constructed using the most parsimonious trees. We also calculated bootstrap support index (Felsenstein 1985) for the branches in consensus tree of MP by running 1000 pseudoreplicates on TNT. For both analyses (BI and MP) we used *Ischnocnema parva* to root the trees since recent molecular studies have established *Ischnocnema* as the sister clade of *Brachycephalus* (Padiál *et al.* 2014).

Taxonomy

Nineteen specimens were found in the Serra Queimada trail (22°19'21.2''S 042°16'19.8''W, 1169 m a.s.l.), APA de Macaé de Cima, Lumiar, municipality of Nova Friburgo, State of Rio de Janeiro, Southeastern Brazil.

Brachycephalus bufonoides Miranda-Ribeiro, 1920

Brachycephalus ephippium var. *bufonoides* Miranda-Ribeiro, 1920.

Brachycephalus ephippium: Cochran, 1955 (part).

Brachycephalus bufonoides: Pombal, 2010.

Lectotype. MZUSP 1459 (designated by Pombal 2010). Type locality: Serra de Macaé, Nova Friburgo, State of Rio de Janeiro, Brazil on September 1909 collected by Ernest Garbe. Paralectotype MZUSP 1458, collected with the lectotype.

Referred specimens. The Serra Queimada trail (22°19'21''S, 42°16'19''W: datum WAG84; 1169 m above sea level), Área de Proteção Ambiental (APA) de Macaé de Cima, municipality of Nova Friburgo, state of Rio de Janeiro, southeastern Brazil: MNRJ 91685 (male) and ZUF RJ 15424–26 (males), 15428–30 (males) collected on 3 October 2015 by M. Folly and L. C. Amaral; and MNRJ 91686 (female), MNRJ 91687–88 (males), ZUF RJ 15525 (male), ZUF RJ 15527 (male), ZUF RJ 15528–29 (females), ZUF RJ 15530–31 (males), ZUF RJ 15534–35 (males), and ZUF RJ 15536 (female) collected on 20 November 2015 by Manuella Folly, Lucas C. Amaral, Sergio P. de Carvalho-e-Silva, and José P. Pombal Jr.

Diagnosis. The specimens show absence of sternum; eight presacral vertebrae; palatal shelf of maxilla lacking pterygoid process; neopalatines and columella absents; arrow-shaped terminal phalanges; one phalange in Finger V, very short phalange in Toe I. These characters have been proposed as diagnostic of *Brachycephalus* (Hedges *et al.* 2008). *Brachycephalus bufonoides* belongs to this genus by the aforementioned characters and also by the small size (<18 mm in both males and females). Furthermore, it is assigned to the *B. ephippium* species group by: (1) bufoniform body shape; and (2) hyperossified skull and presence of hyperossified spinal processes of sacral and presacral vertebrae (intermediate condition *sensu* Clemente-Carvalho *et al.* 2012). Adults of *B. bufonoides* are distinguished from all of its congeners by the combination of the following characters: (1) skin on head and dorsum with dermal hyperossification; (2) skull with hyperossification of postorbital crests; (3) a pair of hyperossified bulges about equidistant between postorbital crests; (4) fourth presacral vertebra with transverse process hyperossified, ornamented and sacral diapophyses hyperossified, which can be seen externally (lineage of *B. vertebralis* *sensu* Condez *et al.* 2020); (5) presence of dermal ossification as separated bulges of each vertebrae; (6) general background color orange with different intensities of dark orange blotches on dorsum, including bordering of sacral region; (7) absence of osteoderms and presence of warts on the dorsolateral surface of body; (8) medium body size (SVL of adults: 12.0–14.5 mm for males and 14.7–16.3 mm for females; Table 1); (9) rough dorsum; (10) advertisement calls with 13 to 17 pulses; (11) presence of pulse period modulation; and (12) advertisement calls with notes longer than 0.2 s (0.22 to 0.31 s).

Comparisons with the other species. *Brachycephalus bufonoides* (Fig. 2) has skin on the head and vertebrae with dermal ossification, and a hyperossified process of the fourth vertebra. These characteristics distinguish the species from *B. pernix* species group (*B. actaeus*, *B. albolineatus*, *B. auroguttatus*, *B. boticario*, *B. brunneus*, *B. coloratus*, *B. curupira*, *B. ferruginus*, *B. fuscolineatus*, *B. izecksohni*, *B. leopardus*, *B. mariaeterezae*, *B. mirissimus*, *B. olivaceus*, *B. pernix*, *B. pombali*, *B. quiririensis*, *B. tridactylus*, and *B. verrucosus*; Pombal *et al.* 1998; Ribeiro *et al.* 2005; Alves *et al.* 2006; Haddad *et al.* 2010; Garey *et al.* 2012; Pie and Ribeiro 2015; Bornschein *et al.* 2016; Monteiro *et al.* 2018a; Ribeiro *et al.* 2017; Pie *et al.* 2018) and from *B. didactylus*, *B. hermogenesi*, *B. pulex*, and *B. sulfuratus* that completely lack hyperossification (Izecksohn, 1971; Giaretta and Sawaya, 1998; Napoli *et al.* 2011; Clemente-Carvalho *et al.* 2012; Condez *et al.* 2016).

TABLE 1. Measurements in millimeters of collected specimens of *Brachycephalus bufonoides*. Abbreviations are mean (\bar{x}); standard deviation (SD); snout–vent length (SVL); axilla–groin length (AGL); head length (HL); head width (HW); nostril diameter (ND); internostril distance (IND); eye diameter (ED); eyelid width (EW); interorbital distance (IOD); eye–nostril distance (END); nostril–tip of snout distance (NSD); thigh length (THL); shank length (SL); foot length (FL); Toe-III length (TL); arm length (AL); forearm length (FAL); hand length (HAL); and Finger-IV length (FIL).

	Males (n=14)			Females (n=4)		
	\bar{x}	SD	Range	\bar{x}	SD	Range
SVL	13	0.7	12.0–14.5	15.5	0.5	14.7–16.3
AGL	4.7	0.9	2.7–6.1	6.3	0.9	5.5–7.8
HL	2.6	0.3	2.2–3.3	3.1	0.2	2.9–3.4
HW	5.5	0.1	5.3–5.7	6	0.1	5.8–6.2
ND	0.4	0.1	0.2–0.5	0.4	0.04	0.4–0.5
IND	1.8	0.1	1.6–2.1	1.9	0.02	1.89–1.95
ED	1.5	0.1	1.2–1.7	1.4	0.05	1.3–1.5
EW	1	0.1	0.8–1.2	1.07	0.05	1.0–1.1
IOD	2.4	0.1	2.1–2.6	2.6	0.05	2.5–2.7
END	0.8	0.1	0.6–1.0	0.8	0.05	0.7–0.9
NSD	0.6	0.1	0.4–0.8	0.6	0.09	0.5–0.7
THL	5.8	0.4	5.0–6.5	6.6	0.2	6.3–6.9
SL	5.5	0.3	5.0–6.2	6.3	0.02	6.3–6.36
FL	7.4	0.3	6.8–7.9	8.3	0.3	7.8–8.8
TL	2.9	0.2	2.3–3.1	3.2	0.1	3.0–3.3
AL	2.6	0.3	1.8–3.2	2.8	0.2	2.4–3.1
FAL	2.9	0.2	2.5–3.3	3.2	0.1	3.1–3.4
HAL	2.6	0.1	2.4–2.9	3	0.06	2.9–3.0
FIL	0.8	0.1	0.7–1.0	0.9	0.08	0.8–1.0

By having a hyperossified dorsal shield or hyperossified spinal process of sacral and presacral vertebrae, *Brachycephalus bufonoides* belongs to *B. ephippium* species group. This species can be distinguished from *B. darkside*, *B. ephippium*, *B. garbeanus*, and *B. margaritatus* by its presence of dermal ossification on the vertebrae (bony shields on dorsum in these species: Pombal 2010; Pombal and Izecksohn 2011; Guimarães *et al.* 2017). *Brachycephalus bufonoides* has a transverse process of the fourth presacral vertebra and sacral diapophyses hyperossified and ornamented, which is very distinct of the large bone plate exhibited by *B. ephippium*, *B. darkside*, *B. garbeanus*, and *B. margaritatus*; and also distinct from the comparatively less ornamented skeleton (intermediate condition *sensu* Clemente-Carvalho *et al.* 2012; *B. vertebralis* lineage *sensu* Condez *et al.* 2020); *B. vertebralis* lineage *sensu* Condez *et al.* 2020 of *B. alipioi*, *B. crispus*, *B. guarani*, *B. nodoterga*, *B. pitanga*, *B. toby*, and *B. vertebralis* (Pombal and Gasparini 2006; Haddad *et al.* 2010; Clemente-Carvalho *et al.* 2012; Condez *et al.* 2014). Absence of osteoderms distinguishes *B. bufonoides* species from *B. crispus*, *B. margaritatus*, and *B. nodoterga*. *Brachycephalus bufonoides* has skin on its head with dermal ossification and the presence of dermal ossification on the vertebrae while *B. atelopoides* has no dorsal shields and cephalic ossification (Miranda-Ribeiro 1920; Pombal 2010). The orange coloration with different intensities of dark orange blotches on the dorsum of *B. bufonoides* differs from *B. alipioi*, *B. pitanga*, *B. guarani*, and *B. toby* (orange uniform in *B. alipioi*: Pombal and Gasparini 2006); orange with red irregular blotches in *B. pitanga* (Alves *et al.* 2009); orange with a dark brown vertebrate stripe in *B. guarani* (Clemente-Carvalho *et al.* 2012); orange with dorsal greenish in *B. toby* (Haddad *et al.* 2010). Further, *B. bufonoides* can be distinguished from *B. crispus* and *B. nodoterga* by its dorsum without dermal ossification like warts on the skin [with ossification is *B. crispus* and *B. nodoterga* (Condez *et al.* 2014)].

Redescription of the species. Measurements for 15 males and four females are given in Table 1. Vocal slits not observed in males; body robust and bufoniform (Figs. 1–3); head wider than long (HL/HW \bar{x} = 0.51 in males and females); head length approximately 19% of SVL in males and 20% in females; snout short with length almost

half of eye diameter ($END/ED \bar{x} = 0.56$ in males and 0.57 in females), rounded in dorsal and lateral views; nostrils, directed anterolaterally, elliptical, not protuberant; *canthus rostralis* distinct, almost straight; loreal region vertical; eye not protruding dorsally, mean of eye diameter 57% of HL in males and 46% in females; tympanum not visible; supratympanic fold absent; a hyperossified postorbital crest; a pair of hyperossified bulges about equidistant between postorbital crest; tongue long and narrow, without indentation on its free posterior border; choanae elliptical, anterior to the eye; vomerine odontophores absent; premaxillary and maxillary teeth absent. Arm slightly shorter than forearm ($AL/FAL \bar{x} = 0.90$ in males and 0.87 in females), slender; total arm length with mean of 42% SVL in males and 39% in females; hands with the same length in males ($AL/HAL \bar{x} = 1.0$) and almost of the same length of upper arm in females ($AL/HAL \bar{x} = 0.95$); Finger III and IV robust, distinct; IV longer than III; Finger II very short and Finger V vestigial; pointed tip of Finger III and IV; subarticular tubercles, inner, and outer metacarpal tubercles absent. Shank as long as thigh ($SL/TL \bar{x} = 0.96$ in males and 0.95 in females); total leg length with mean of 84% of SVL in both males and females; thigh length larger than foot length ($TL/FL \bar{x} = 0.78$ in males and 0.80 in females); Toe II, III, and IV distinct, robust; Toe I and V reduced; tip of Toe II rounded, tip of Toe III and IV pointed; relative length of toes $I \approx V < II < III < IV$; subarticular, inner and outer metatarsal tubercles absent. Skin on head, vertebral column and fourth vertebra with dermal hyperossifications; skin on dorsolateral surface of body, flanks, and dorsal surface of thighs granular; presence of warts on the dorsolateral surface of body; skin on venter and ventral surfaces of the legs smooth; granular skin on ventrolateral surfaces of body and area around the cloacal opening.



FIGURE 1. *Brachycephalus bufonoides* (ZUF RJ 15525) in life.

Coloration in life. General background coloration orange; dorsum with a dark orange blotch bordering the spine; protruding dorsal hyperossifications lighter orange than the dorsum color (Fig. 1); finger IV and toe V with black tips; a light-yellow line below the eye, eye black in color. Dorsum varies from orange to light orange blotches bordering to the spine varying in different intensities.

Coloration in preservative and variation. Upper surfaces gray (Figs. 3A–D); protruding dorsal hyperossifications beige (Fig. 3E), flanks light brown; tips of Finger IV and toe V gray; a cream line below the eyes. Dorsal surfaces of body can be gray to brown, varying specially from below the head to the cloaca. In robust specimens, the ossified structures on the head, dorsum and diapophyses are less distinct (Fig. 3D) than thinner specimens that have such ossified structures much evident (Figs. 3A, C). The hyperossification in the spinal processes of presacral vertebrae is completely ossified forming an irregular (MNRJ 91688 and MNRJ 91687) or regular oval shape (ZUF RJ 15428 and ZUF RJ 15529).

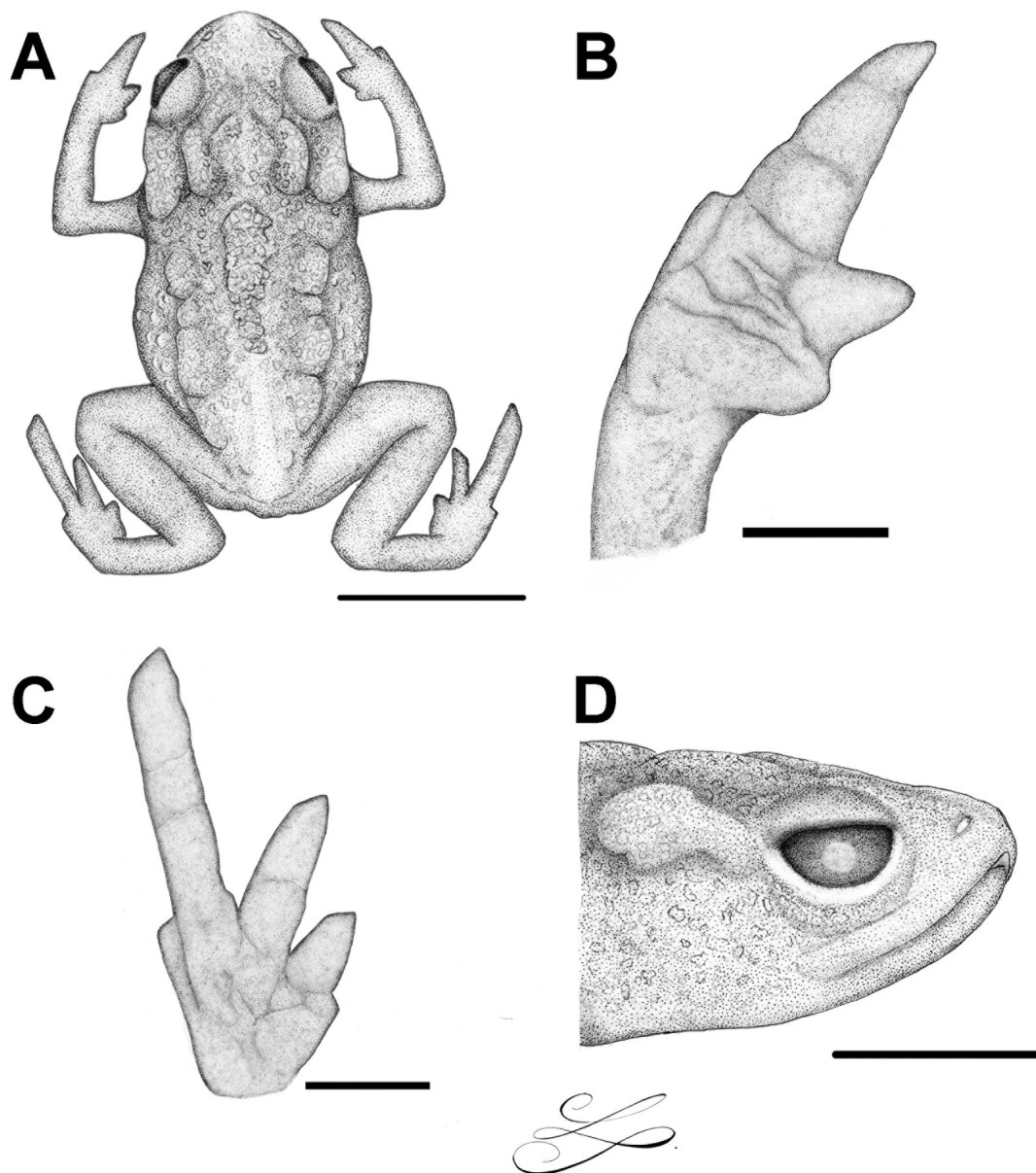


FIGURE 2. *Brachycephalus bufonoides* (ZUFRJ 15525). Dorsal view of the body (A), ventral views of the right hand (B), the right foot (C), and lateral view of the head (D). Scale is 5 mm.

Natural history. Specimens of *Brachycephalus bufonoides* were active during the day were found on forest floor or amidst leaf litter. Some individuals were found under fallen tree trunks where the moisture is higher. Specimens were observed walking slowly on the leaf-litter. Generally, males were observed and heard calling under the leaves of the leaf-litter or branches, but they can be found calling exposed on the surface of leaf-litter or timber (males observed on cloudy and rainy days). Individuals were seen calling from both above and under the leaf-litter, except for one individual, which was calling on a fallen tree trunk.

Vocalizations. The individuals found calling in the field were recorded at air temperature of 20.8 °C, and relative humidity of the air of 78%. Calls were emitted as a regular series of low-intensity buzzes (around 120 dB at about 1-meter recording distance). The advertisement call duration is of up to 3 minutes (specimens usually stopped calling when disturbed), and consists of a series of regularly emitted notes, with constant general amplitude (Fig. 4). Notes consisted of a number of pulses, ranging from 13 to 17 pulses/note ($\bar{x} = 15.05 \pm 0.88$; $\tilde{x} = 15$; Mo = 16; $n = 352$), with most of them consisting of 14 to 16 pulses (96.7%). Amplitude modulation increased until the second quarter, with a mild descending modulation from end of second quarter until the end of the note. Note duration ranges from 222.09 to 308.53 ms ($\bar{x} = 271.33 \pm 18.70$; $\tilde{x} = 276.00$; Mo = 290.07; $n = 352$). Inter-note interval duration

ranges from 147.58 to 265.00 ms (\bar{x} = 209.05 ± 24.68; \tilde{x} = 219.00; Mo = 232.00; n = 298). Note period ranges from 401.82 to 545.00 ms (\bar{x} = 482.10 ± 35.61; \tilde{x} = 495.00; Mo = 503.00; n = 298). Note repetition rate ranges from 1.98 to 2.43 note/s (\bar{x} = 2.15 ± 0.20; \tilde{x} = 2.04; n = 3). Pulse period ranges from 9.89 to 25.13 ms (\bar{x} = 18.18 ± 3.39; n = 729). There is a pulse period modulation to shorter duration of the periods starting through the second third of the note, and continuing modulation to longer duration of the periods through the final third of the note. Pulse repetition rate ranges from 47.55 to 71.28 pulses/s (\bar{x} = 56.20 ± 4.81; \tilde{x} = 55.01; Mo = 51.27; n = 352). Pulse envelope with decay steeper than attack. Dominant frequency of the call ranges from 4.13 to 4.88 kHz (\bar{x} = 4.55 ± 0.14; \tilde{x} = 4.5; Mo = 4.5; n = 344); minimum frequency ranges from 2.49 to 4.24 kHz (\bar{x} = 3.38 ± 0.37; \tilde{x} = 3.43; Mo = 3.37; n = 98), and maximum frequency ranges from 5.58 to 7.05 kHz (\bar{x} = 6.268 ± 0.37; \tilde{x} = 6.25; Mo = 5.94; n = 98).

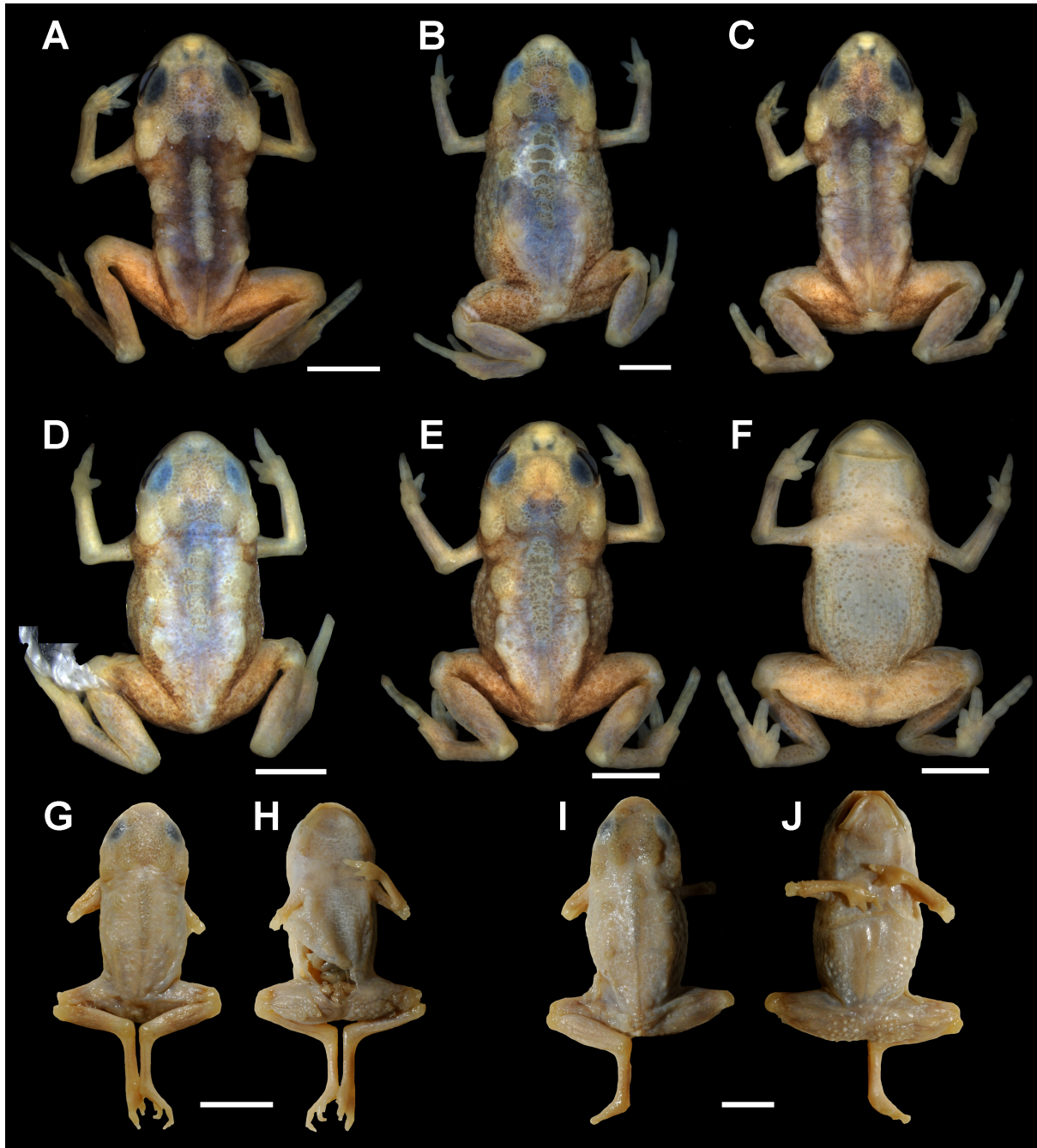


FIGURE 3. Variation in preserved specimens of *Brachycephalus bufonoides*. (A) ZUF RJ 15428 (male; SVL 13.6 mm), (B) ZUF RJ 15529 (female; SVL 16.3 mm), (C) MNRJ 91688 (male; SVL 12.0 mm), (D) MNRJ 91687 (male; SVL 13.0 mm), (D–E) ZUF RJ 15525 (male; SVL 14.1 mm) in dorsal and ventral views, (G–H) *B. bufonoides* lectotype (MZUSP 1459; SVL 13.5 mm) in dorsal and ventral views and, (I–J) *B. bufonoides* paralectotype (MZUSP 1458; SVL 16.4 mm) in dorsal and ventral views. Scale bar = 3 mm.

Comparison with advertisement calls of species of *Brachycephalus*. *Brachycephalus bufonoides* differs from the other species of *Brachycephalus* by a number of distinct advertisement call parameters. *Brachycephalus bufonoides* has greater number of pulses (range = 13–17) than the species belonging to the *B. pernix* group: *B. actaeus* 2–3 pulses (Monteiro *et al.* 2018a); *B. albolineatus* 1–3 pulses (Bornschein *et al.* 2017); *B. mirissimus* 1–3 pulses (Pie *et al.* 2018); *B. olivaceus* 2–3 (Monteiro *et al.* 2018b); *B. pernix*: 3 pulses (Wistuba 1998); *B. quiririensis* 3–4 pulses (Monteiro *et al.* 2018b); *B. tridactylus* 1 pulse (Garey *et al.* 2012), and also presents longer note duration in *B. bufonoides*: \bar{x} = 271.33 ms, while in *B. actaeus* \bar{x} = 4 ms (Monteiro *et al.* 2018a); *B. albolineatus* \bar{x} = 20 ms (Bornschein *et al.* 2017); *B. olivaceus* \bar{x} = 38 ms (Monteiro *et al.* 2018b); *B. pernix* \bar{x} = 60 ms (Wistuba 1998); *B. quiririensis* \bar{x} = 50 ms (Monteiro *et al.* 2018b); *B. tridactylus* \bar{x} = 110 ms (Garey *et al.* 2012). It also differs acoustically from most of them by presenting shorter inter-note interval in *B. bufonoides* \bar{x} = 0.27 s, while in *B. actaeus* \bar{x} = 5.42 s (Monteiro *et al.* 2018a); *B. albolineatus* \bar{x} = 6.66 s (Bornschein *et al.* 2018); *B. mirissimus* \bar{x} = 5.83 s (Pie *et al.* 2018); *B. olivaceus*: \bar{x} = 10.69 s (Monteiro *et al.* 2018b); *B. quiririensis*: \bar{x} = 12.58 s (Monteiro *et al.* 2018b), and lower dominant frequency in *B. bufonoides* \bar{x} = 4.6 kHz, while in *B. actaeus* \bar{x} = 6.9 kHz (Monteiro *et al.* 2018a); *B. albolineatus* \bar{x} = 6.4 kHz (Bornschein *et al.* 2018); *B. mirissimus* \bar{x} = 6.7 kHz (Pie *et al.* 2018); *B. olivaceus*: \bar{x} = 6.8 kHz (Monteiro *et al.* 2018b); *B. quiririensis* \bar{x} = 6.3 kHz (Monteiro *et al.* 2018b). The dominant frequency of *B. tridactylus* \bar{x} = 4.8 kHz (Garey *et al.* 2012) overlaps with the range of *B. bufonoides* (4.1–4.9 kHz), and so does *B. pernix* 4.5–6.7, \bar{x} = 5.6 kHz (Wistuba 1998). Values for pulse repetition rate and note repetition rate also vary greatly.

The species from *Brachycephalus ephippium* group have an overall similar structure of the call, consisting in constant repetition of pulsed notes. *Brachycephalus bufonoides* can be distinguished from the other species of the *B. ephippium* group by a combination of different call structures. It differs most from *B. darkside* for presenting greater number of pulses (*B. bufonoides* 13–17 pulses, \bar{x} = 15) in *B. darkside* 5–8 pulses, \bar{x} = 6 (Guimarães *et al.* 2017), while is similar or overlaps parts of the range with the other species: *B. crispus* 7–12 pulses, \bar{x} = 10 (Condez *et al.* 2014); *B. ephippium* 5–15 pulses, \bar{x} = 12 (Pombal *et al.* 1994); *B. pitanga*: 7–14 pulses, \bar{x} = 11 (Araújo *et al.* 2012; Tandel *et al.* 2014). The note duration also is close to or overlaps some of its range with two of the species (*B. bufonoides*: 221–309, \bar{x} = 271 ms); *B. crispus* \bar{x} = 280 ms (Condez *et al.* 2014); *B. pitanga*: 150–250, \bar{x} = 190 ms (Tandel *et al.* 2014), \bar{x} = 170 ms (Araújo *et al.* 2012), but the value is lower in *B. darkside* \bar{x} = 111 ms: Guimarães *et al.* 2017) and *B. ephippium* (\bar{x} = 112 ms: Pombal *et al.* 1994). The interval between notes of *B. bufonoides* (148–265, \bar{x} = 209 ms) differs mostly from that of *B. crispus* (\bar{x} = 350 ms: Condez *et al.* 2014), but overlaps slightly with the other species (*B. darkside* 122–215, \bar{x} = 159.5 ms: Guimarães *et al.* 2017); *B. ephippium* (123–149, \bar{x} = 134 ms: Pombal *et al.* 1994); *B. pitanga* (200–430, \bar{x} = 280 ms: Tandel *et al.* 2014). The pulse repetition rate (\bar{x} = 56.20 pulses/s in *B. bufonoides*) is distinct from that of *B. crispus* \bar{x} = 17.4 pulses/s: Condez *et al.* 2014) but is similar to the rate of *B. darkside* \bar{x} = 56.9 pulses/s: Guimarães *et al.* 2017) and *B. pitanga* \bar{x} = 62.4 pulses/s: Araújo *et al.* 2012). Furthermore, note repetition rate of *B. bufonoides* (\bar{x} = 2.15 notes/s, or 129 notes/min) is similar to the rate of *B. crispus* \bar{x} = 1.67 notes/s: Condez *et al.* 2014) and *B. pitanga* \bar{x} = 159 notes/min: Araújo *et al.* 2012) but differs from that of *B. darkside* \bar{x} = 211 notes/min: Guimarães *et al.* 2017). *Brachycephalus bufonoides* can be further distinguished from *B. darkside* for its higher dominant frequency (*B. bufonoides*: 4.1–4.9 kHz, \bar{x} = 4.6 kHz) while in *B. darkside*: 2.8–3.8 kHz (Guimarães *et al.* 2017), but differ less from the other species (*B. ephippium*: \bar{x} = 3.9 kHz (Goutte *et al.* 2017), lowest frequency = 3.4 kHz, highest frequency = 5.3 kHz (Pombal *et al.* 1994), and overlaps with the range of *B. crispus*: \bar{x} = 4.6 kHz: Condez *et al.* 2014 and *B. pitanga*: \bar{x} = 4.9 kHz (Araújo *et al.* 2012) and \bar{x} = 4.8 kHz (Tandel *et al.* 2014).

The advertisement call of *B. hermogenesi* (\bar{x} = 6.8 kHz: Verdade *et al.* 2008) and *B. sulfuratus* (\bar{x} = 6.7 kHz: Condez *et al.* 2016) differ from *B. bufonoides* by presenting higher dominant frequency. Some overlap between the note duration of *B. sulfuratus* (131–233, \bar{x} = 195 ms: Condez *et al.* 2016) and *B. bufonoides* (221–309 ms) was noticed, however a greater number of pulses per note in *B. bufonoides* (\bar{x} = 15 pulses) than in *B. sulfuratus* 7–11 pulses, \bar{x} = 9 (Condez *et al.* 2016) was observed, which results in difference in the pulse rate between *B. bufonoides* (\bar{x} = 56.2 pulses/s) and *B. sulfuratus* (6.1–12.3, \bar{x} = 9.3 pulses/s: Condez *et al.* 2016). The note repetition rate of *B. bufonoides* (\bar{x} = 2.15 notes/s) is greater than *B. hermogenesi* (\bar{x} = 1.09 notes/s: Verdade *et al.* 2008). Furthermore, even though the values were not given by Verdade *et al.* (2008), the analyzing the graphs provided, *B. hermogenesi* seems to also differ in number of pulses per note, its repetition rate, and other parameters.

Type locality and distribution. *Brachycephalus bufonoides* was originally collected from Serra de Macaé region (Miranda-Ribeiro 1920) which was attributed to the municipality of Nova Friburgo and mountain range of municipality of Macaé, State of Rio de Janeiro (IBGE 1959). Bokermann (1966) attributed the type-locality of *B. bufonoides* to the municipality of Nova Friburgo, State of Rio de Janeiro, Brazil. A report presented by Ihering and Ihering (1911) on expeditions made by Museu Paulista (where E. Garbe worked) between 1906 and 1909, simply states the year and general locality names. Labels of bird specimens collected by E. Garbe in this same expedi-

tion also failed to provide further information (L.F. Silveira, *pers. comm.*). Perhaps, nowadays it is impossible to determine the precise locality (or localities) where *B. bufonoides* was collected by E. Garbe. The Área de Proteção Ambiental (APA) de Macaé de Cima, municipality of Nova Friburgo, state of Rio de Janeiro (Fig. 5), where the specimens of *B. bufonoides* were now collected (present study), is recognized as inserted in Serra de Macaé, the same mountain range of the type-locality of *B. bufonoides*.

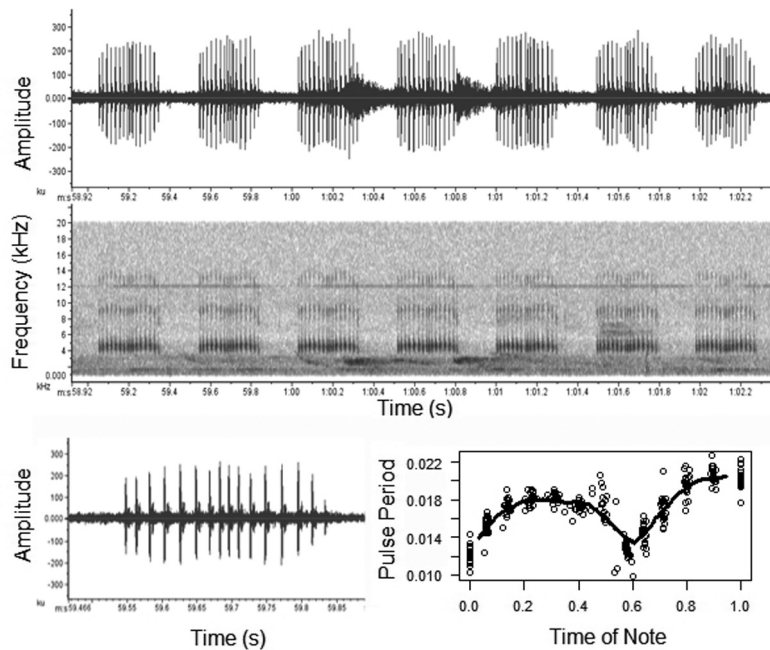


FIGURE 4. Advertisement call of *Brachycephalus bufonoides* (adult male, ZUF RJ 15425) from Área de Proteção Ambiental (APA) de Macaé de Cima, municipality of Nova Friburgo, state of Rio de Janeiro, Brazil. Oscillogram (above) and spectrogram (middle) of sequence of seven notes. Band filter of 1000 Hz applied. Oscillogram of a note (left below). Notice the slight change in pulse period and amplitude throughout the note. Scatterplot (right below) depicting the pulse period modulation in 21 notes, with line representing a moving average tendency line (rolling window = 45). *X-axis*: Time of Note not in seconds but normalized.

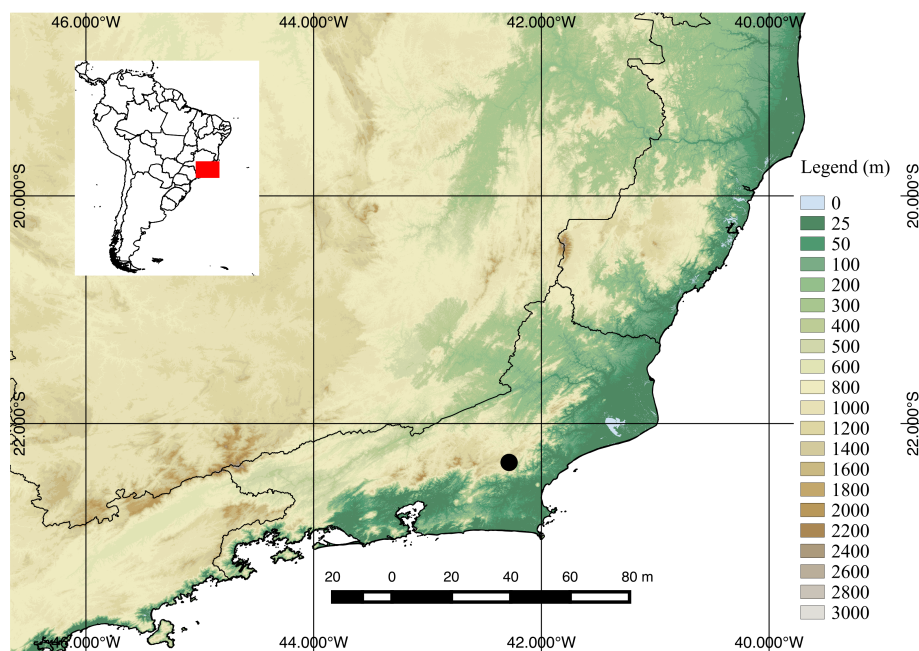


FIGURE 5. Geographic location of recent collected specimens of *Brachycephalus bufonoides*. Área de Proteção Ambiental (APA) de Macaé de Cima, municipality of Nova Friburgo, center of the state of Rio de Janeiro, Brazil.

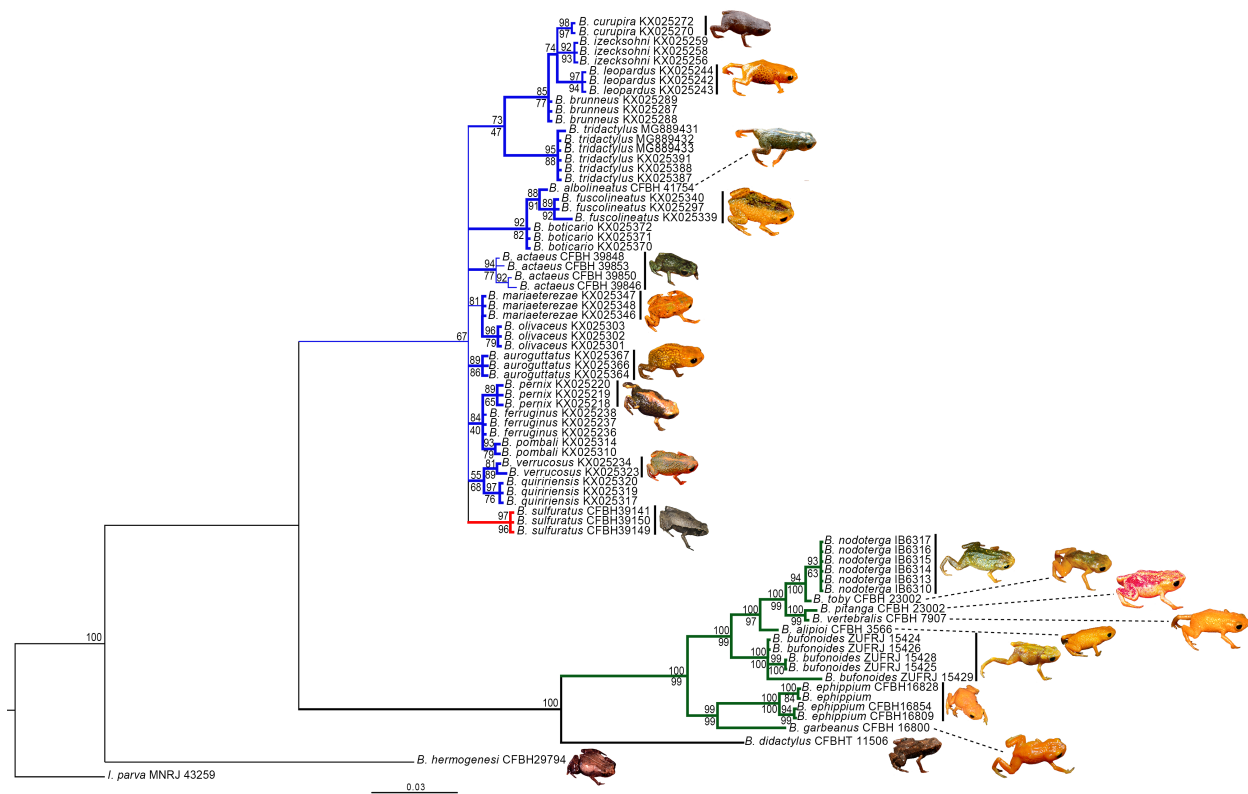


FIGURE 6. Bayesian Inference tree (lnL = -4368.48) for 16S sequences (999 aligned basepairs, 78 terminals; 2 partitions = for the two fragments: each GTR+G) of species of *Brachycephalus*. Thicker clades refer to those also found by maximum parsimony. Clade support values include posterior probabilities above branches and parsimony bootstrap below branches. Branches were colored according to their classification into *B. pernix* (blue), and *B. ephippium* (green), according to Ribeiro *et al.* (2015). Photos provided by C. de Luna-Dias (*B. ephippium*), R. Sawaya (*B. nodoterga* and *B. hermogenesi*), and C.F.B. Haddad (*B. vertebralis*). Photos modified of Alves *et al.* (2009) (*B. pitanga*), Haddad *et al.* (2010) (*B. toby*), Condez *et al.* (2016) (*B. sulfuratus*), Ribeiro *et al.* (2015) (*B. auroguttatus*, *B. fuscolineatus*, *B. leopardus*, *B. mariaeterezae*, and *B. verrucosus*), Bornschein *et al.* (2016) (*B. albolineatus*), Ribeiro *et al.* (2017) (*B. coloratus*), and Monteiro *et al.* (2018a) (*B. actaeus*).

Molecular analysis. Considering DNA sequences of the 16S gene (999 aligned basepairs, 78 terminals), the topology generated, on the basis of both phylogenetic analyses (BI and MP), supported the recognition of *Brachycephalus bufonoides* and of *B. ephippium* species group (specimens appear clustered into eight exclusive lineages, which are supported by high posterior probability and bootstrap values (Fig. 6), that corroborates the morphological identification.

Furthermore, the population of *Brachycephalus bufonoides* was recovered as a monophyletic group. The genetic distances between this species and the sister clade composed by *B. alipioi*, *B. pitanga*, *B. vertebralis*, *B. toby*, and *B. nodoterga* range from 3.2–5.8%, corroborating the distinction between these species. We found low genetic distances among four of five analyzed specimens (ZUF RJ 15424, 15426–28) of *B. bufonoides*, with maximum values corresponding to 0.001% between the specimen from Serra Queimada trail, APA de Macaé de Cima, Lumiar, municipality of Nova Friburgo, RJ. However, the specimen ZUF RJ 15429 had the value between 0.021 and 0.022% of distance from the other four specimens.

Osteology of *Brachycephalus bufonoides*

Skull (Figs. 7–8)

Shape and proportions. The skull is wider than long (length/width range 74–84%, $N = 3$). The length of the orbit is about half the total length of the skull (orbit/length 47–59%). The skull is widest at the prootics, and the jaw articulation lies well anterior of the posterior end of the skull on the occipital condyles. The jaws are relatively short,

with the posterior apex lying to the level of the optic fenestra. Dermal roofing bones of the skull ornamented with co-ossification of skin to bones. Nasal, sphenethmoid, frontoparietals, prootics, and exoccipitals are synostosed, hyperossified and sculptured forming a dorsal cranial plate.

Dermal investing bones. *Nasals* – sculptured. These bones are completely synostosis with sphenethmoid. An attenuate maxillary process is not in contact with the preorbital process of the pars facialis of the maxilla. ZUFJRJ 15536 has no sculpture on the nasal bone. *Frontoparietals* – hyperossified and sculptured. The paired frontoparietals overlie the taenia tecti marginalis of the braincase. The bones are synostosed medially and completely obscure the frontoparietal fontanelle. Frontoparietals are also synostosed with nasals, sphenethmoid and fused exoccipitals and prootics.

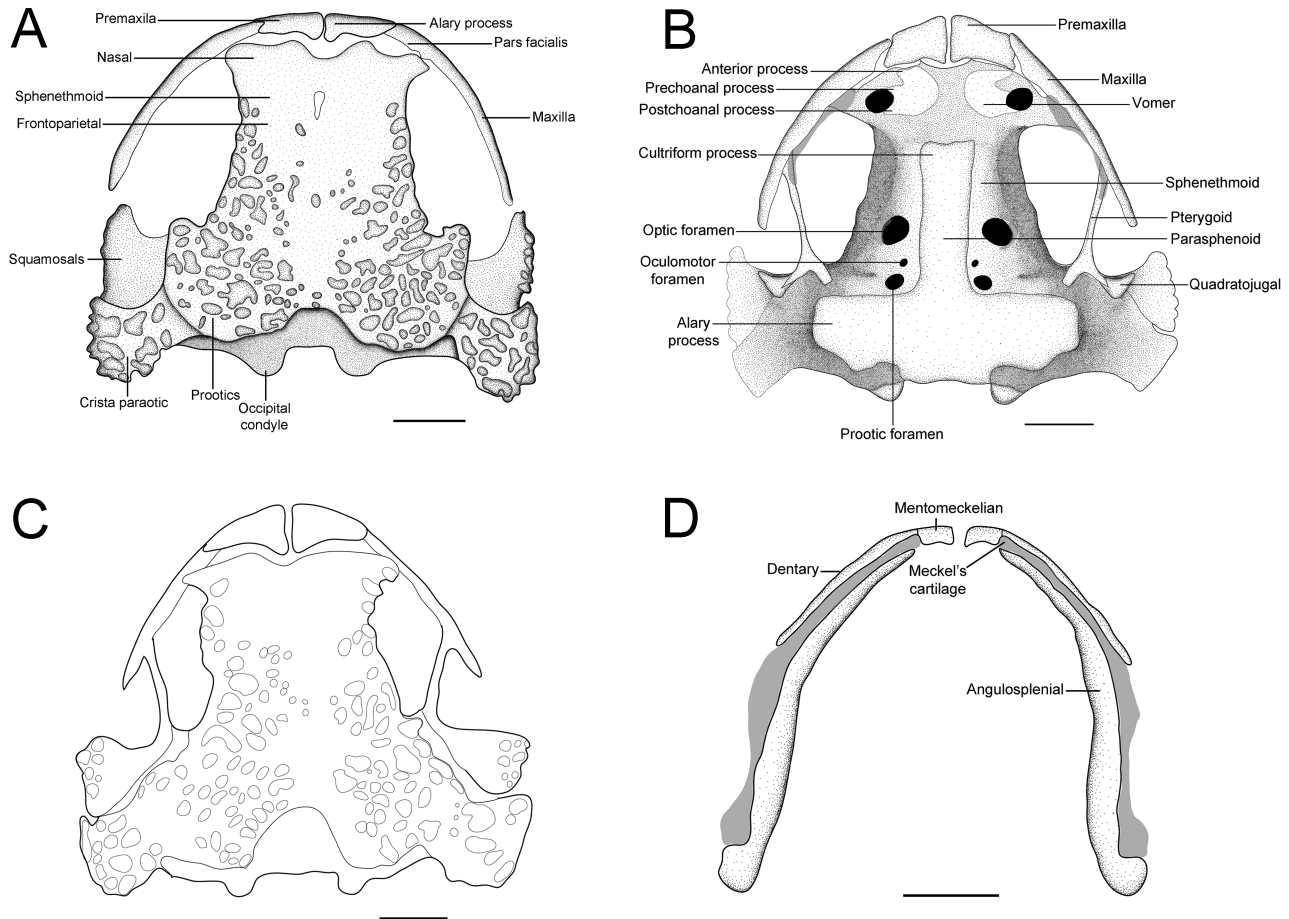


FIGURE 7. Skull of *Brachycephalus bufonoides*. (A) dorsal and (B) ventral views (ZUFJRJ 15536), (C) variation of dorsal view (ZUFJRJ 15535), and (D) mandible (ZUFJRJ 15535). Scale bar: 1 mm.

Neurocranium. *Sphenethmoid* – hyperossified and sculptured. This bone is fused with frontoparietals and nasals. The optic fenestra cartilage is absent. The sphenethmoid of two specimens (ZUFJRJ 15536 and ZUFJRJ 15535) is not sculptured. *Fused Exoccipitals and Prootics* – hyperossified and sculptured. The exoccipital portions of this composite element form the posterior end of the braincase. The prootic portion of the bone forms the posterolateral walls of the braincase and, together with its cartilaginous crista parotica, the middle ear; the head of the squamosal articulates with the lateral margin of the crista parotica. The epiotic eminence (anterior and posterior) is indistinguishable.

Ventral investing bones. *Parasphenoid* – The cultriform process is synostosed with sphenethmoid. The parasphenoid alae are broad and posterolaterally oriented beneath the otic capsule; the distal margins of the alae are truncate and terminate after the midpoint of the otic capsule where almost contact the medial process of the pterygoid. The parasphenoid terminates in a broad truncate or triangular (MZUSP 1459) posteromedial process lying or not (MZUSP 1459) the foramen magnum. *Neopalatine* – absent. *Vomers* – reduced. The anterior process is curved, rounded and extends toward the maxilla. The reduced prechoanal process forms the anterior and anteromedial mar-

gin of the choana and terminates in a rounded point. The postchoanal process forms the posteromedial margin of the choana. The posteromedial margins of the vomers are moderately separated from each other, diverging abruptly anteriorly. The pre- and postchoanal processes are around the same length. The specimen (ZUFRJ 15535) has broad separation between vomers. ZUFRJ 15536 has greater length of all three processes than ZUFRJ 15430 and 15535. The dentigerous process is absent.

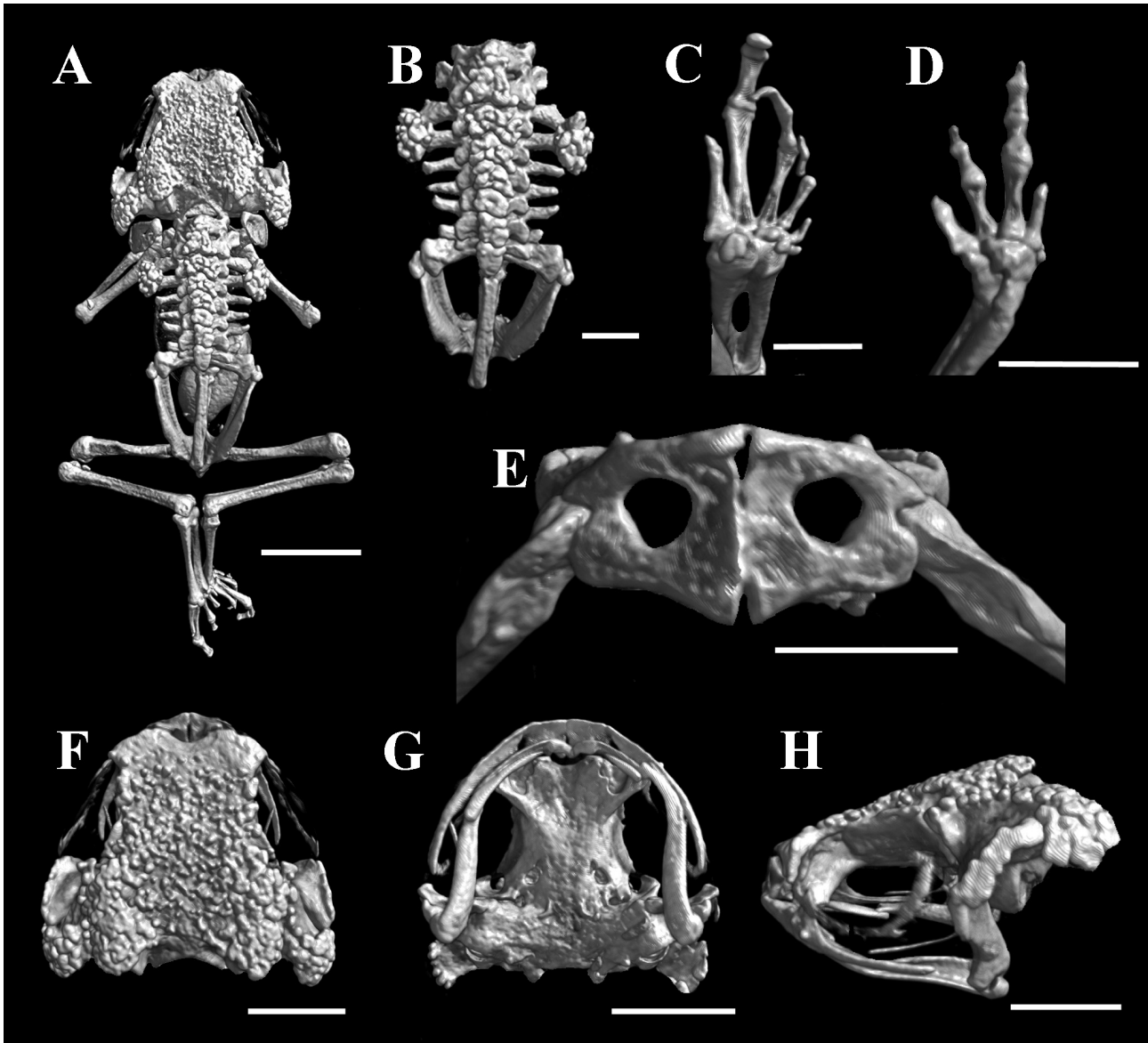


FIGURE 8. High-resolution computed tomography (Micro-CT) scans of the lectotype of *Brachycephalus bufonoides* (MZUSP 1459) showing osteological features. (A) Dorsal view of the skeleton and (B) vertebral column; (C) right foot in plantar view; (D) left hand in palmar view; (E) pectoral girdle in ventral view; (F) dorsal, (G) ventral, and (H) lateral views of the skull (with the lower jaw). Scale bars equal 5 mm.

Maxillary arcade. *Premaxillae* –Each premaxilla is broad and are separated from each other by a short space in front view. The pars dentalis of each premaxilla is lacking. In front view, the height of the alary process corresponds to half the length of premaxillae, and the distal tip of each alary process is bifurcate (“U”-shape). The basal parts of the alary processes converge medially. The distal tips diverge from one another. Laterally, the alary processes are curved. The distal end of each pars palatina is sharp and converges to each other almost touching one another. *Maxillae* –The anterior end of the maxilla overlaps the posterolateral end of the premaxilla. The posterior end of the maxilla is sharp; and does not have teeth. The pars facialis is high, thin and reduced, extending for about half the length of the maxilla. *Quadratojugals* – absent.

Suspensory apparatus. *Pterygoids* –The anterior ramus of each pterygoid is long; cylindrical; terminated in a truncate point; and extends to the median margin of the maxilla. The medial ramus is short; slightly laminar; has a truncated end; and invests the prootic. The posterior ramus is short; triangular; has a sharp point. *Squamosals* –They are composed of three rami that give to the squamosal a “L” shape: the ventral ramus, the otic ramus (posterior ramus) and the zygomatic ramus (anterior ramus). The ventral ramus is the longest of the three, and has a truncated distal end, which is wider than the proximal portion. In lateral view, the zygomatic ramus is shorter than the ventral ramus and the distal end is sharp or rounded (MZUSP 1459), toward to the maxilla, but does not contact it. In lateral view the otic ramus is shorter than the zygomatic ramus, and the distal end is rounded. In dorsal view, the distal end of the otic ramus is truncated, toward the parotic plate, but does not overlap it. *Mandible* –The mentomeckelian bones are located in the anterior part of the mandible and are separated from each other by a short space. In frontal view, the mentomeckelians have a sharp point anteriorly. They are fused to the dentaries laterally. Each dentary invests laterally less than half of the angulosplenic bone and has a pointed posterior end. They do not overlap the Meckel’s cartilage anterolaterally. Angulosplenic bones situated in the lateroposterior part of the mandible in ZUFJR 15430 and 15535, corresponding to about 80% of the lower jaw’s length. ZUFJR 15536 have longer angulosplenic corresponding to around 90% of lower jaw’s length. The anterior end of each angulosplenic is roundly pointed, and the posterior end is robust and rounded. The posterior end of the angulosplenic bears well-developed pars articularis process.

Hyolaryngeal Skeleton (Fig. 9)

Hyoid plate is rectangular *i.e.*, longer than wide. Length of hyoid plate around four times its smallest width. Anterior processes long and straight, forming a deep hyoglossal sinus, which deepens to nearly the height of the alary processes. Alary and posterolateral processes much reduced. Posteromedial processes diverging widely to embrace a broad larynx. Arytaenoids of cricoid are short, semicircular and narrowly separated from each other. Cricoid with short oesophageal process. Laterally contiguous with the posteromedial process, the lateral process of the cricoid fitting over the end of the posteromedial process.

Postcranium

Pectoral girdle (Fig. 10A). Clavicle, coracoid, and scapula fused and completely ossified; procoracoid and epicoracoid fused with coracoid but separated from the clavicle by large fenestrae; suprascapula not expanded, anterior half ossified as cleithrum; omosternum not visible and sternum absent.

Vertebral column (Figs. 10B–D). Vertebral column composed by eight presacral, non-imbricate vertebrae. First presacral vertebra (atlas) lacks transverse process; transverse of Presacrals II–IV bears moderately stout processes, and Presacrals V–VIII are shorter, less robust processes. Transverse processes of Presacrals III–VI perpendicular to the notochordal axis, those of the Presacrals II, VII–VIII directed anteriorly and of the Presacrals V–VI directed posteriorly. Lengths of the transverse process of presacrals along with that of the sacral diapophyses: IV > SD > III > V > VII > VI > II–VIII. Fourth presacral vertebra with transverse process hyperossified and ornamented which can be seen externally. Sacral diapophyses moderately expanded and directed posteriorly, distal end of diapophyses with a flat, slightly calcified cartilage that articulates with the ilial shaft of the pelvic girdle. Sesamoids on both sides of sacral diapophyses can be seen externally. There are two types of bony elements associated with the vertebral column: (1) spinal plates - lies dorsal to the vertebra. All vertebrae have distinct spinal plates, except for Presacrals I and II that have fused spinal plates. (2) ZUFJR 15535 and 15430 also have spinal plates above the sacrum (absent in ZUFJR 15536); and, (2) the paravertebral plates - associated with the transverse processes of vertebrae IV.

Manus (Fig. 11A). Phalangeal formula of the hand 1–2–3–1. The carpus is composed of a radiale, ulnare, element y fused with Carpal 2, and a large postaxial assumed to represent a fusion of centrale with Carpals 3–5. Prepollex with two elements ossified and very reduced. Tips of the terminal phalangeal elements of fingers arrow-shaped (Fig. 10A). One sesamoid occurring at level of the basis of metatarsal V in ZUFJR 15536.

Pes (Fig. 11B). Phalangeal formula of foot 1–2–3–4–1. Tarsus (Fig. 10B) composed of tibiale, fibulare, three individual elements, including distal tarsal 2–3, distal tarsal 1, element y. Distal tarsal 1 is the smallest and articulates with element y, distal tarsal 2–3 and metatarsal I and II. Distal tarsal 2–3 articulates mainly with metatarsal III, also with metatarsal II and IV and with distal tarsal I. There are 2 small sesamoids under the tarsals. Prehallux has one very reduced element. Tips of the terminal phalangeal elements of toes II–IV arrow-shaped, toes I and V reduced with tips of terminal phalangeal elements pointed, elongate on digit IV.

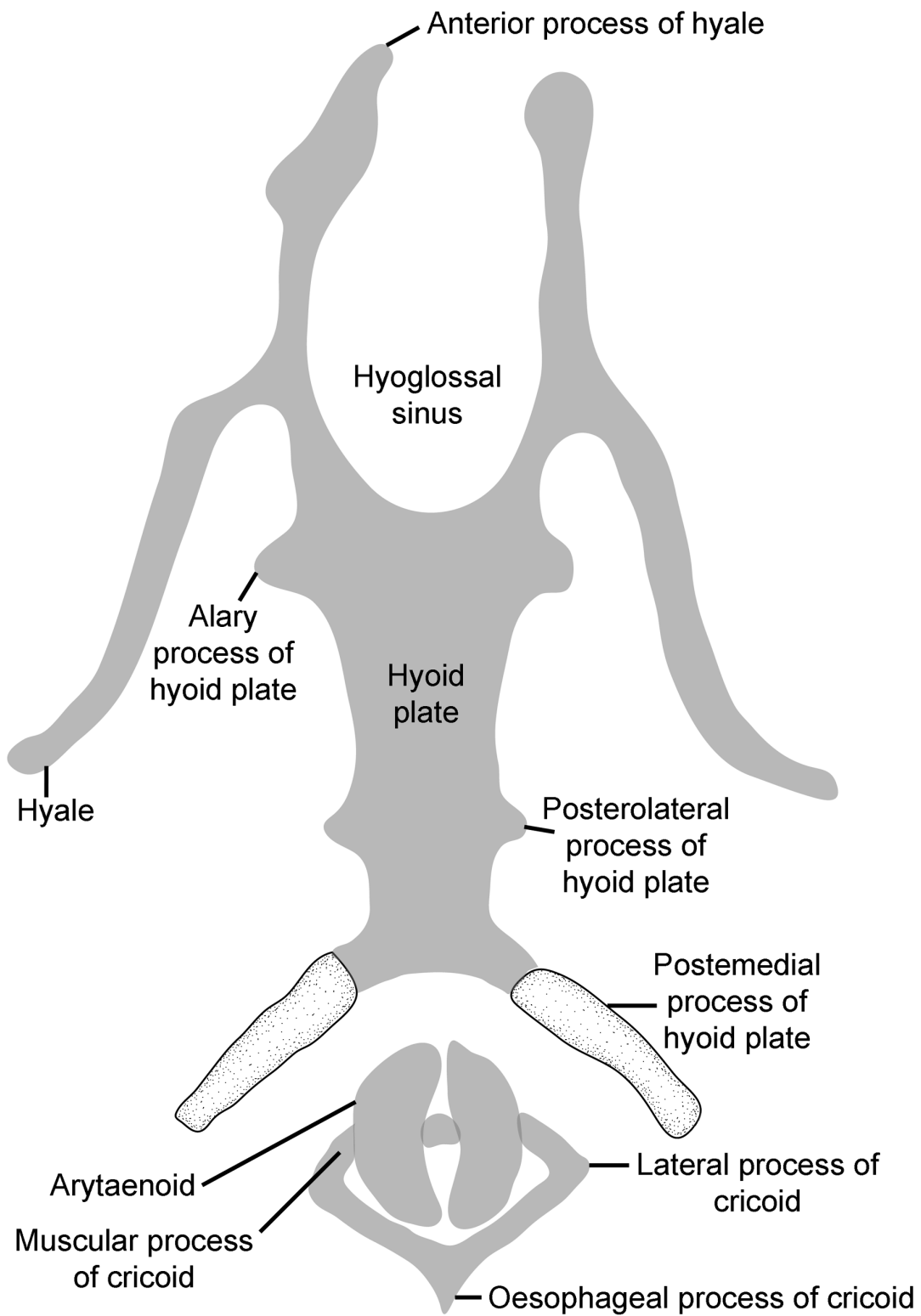


FIGURE 9. Hyolaryngeal skeleton of *Brachycephalus bufonoides* in ventral view (ZUF RJ 15535). Scale bar: 1 mm.

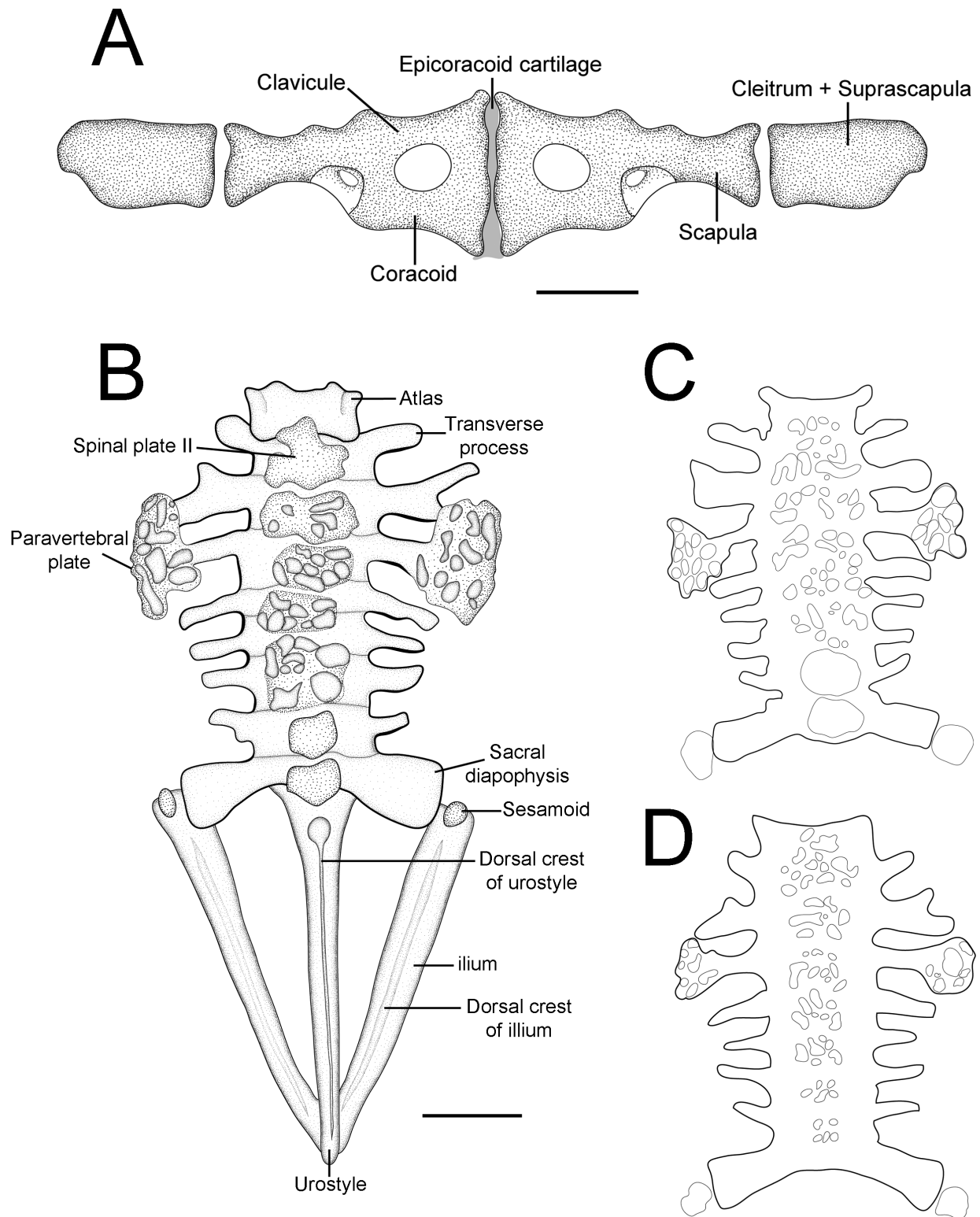


FIGURE 10. Postcranium of *Brachycephalus bufonoides*. (A) Pectoral girdle in dorsal view (ZUFJRJ 15536); (B–D) vertebral column in dorsal view (ZUFJRJ 15430, ZUFJRJ 15535 and ZUFJRJ 15536, respectively). Scale bar: 1 mm.

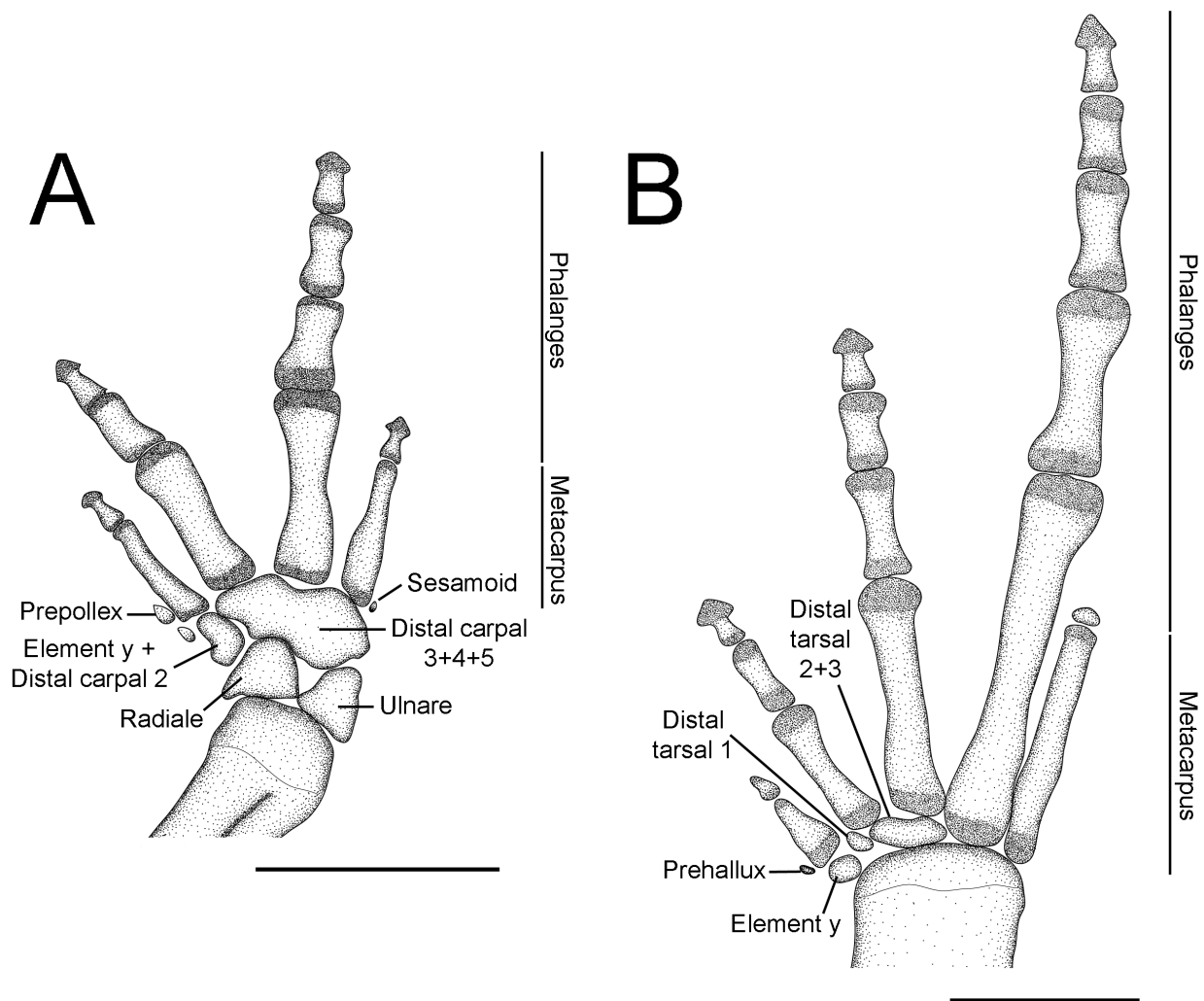


FIGURE 11. *Manus* and *pes* of *Brachycephalus bufonoides* (ZUF RJ 15535). (A) Dorsal views of *manus* and (B) *pes*. Scale bar: 1 mm.

Osteological comparisons of species of *Brachycephalus*. Trends of reduction and loss of skull bones were observed among groups of species in *Brachycephalus*. Among these reductions and losses, columellae are always absent in all analysed species. Species of *B. pernix* group have: (1) reduced neopalatines in *B. albolineatus* (Bornschein *et al.* 2016), *B. brunneus* (Ribeiro *et al.* 2005), *B. coloratus* and *B. curupira* (Ribeiro *et al.* 2017) and *B. izecksohni* (Ribeiro *et al.* 2005) or absence of neopalatines in *B. actaeus* (Monteiro *et al.* 2018a), *B. ferruginus* and *B. pombali* (Alves *et al.* 2006); (2) quadratojugals present in *B. actaeus*, *B. albolineatus*, *B. coloratus*, *B. curupira*, *B. ferruginus*, *B. pombali*, *B. brunneus*, *B. izecksohni*, and *B. pernix* (Ribeiro *et al.* 2005; Alves *et al.* 2006; Bornschein *et al.* 2016; Ribeiro *et al.* 2017; Monteiro *et al.* 2018a); (3) maxillary odontoids present, few in number (6-8) in *B. actaeus*, *B. brunneus*, *B. curupira*, *B. ferruginus*, *B. izecksohni*, *B. pernix* and *B. pombali* (Ribeiro *et al.* 2005; Alves *et al.* 2006; Ribeiro *et al.* 2017; Monteiro *et al.* 2018a) or absent in *B. coloratus* (Ribeiro *et al.* 2017); (4) vomers reduced in *B. actaeus*, *B. brunneus*, *B. curupira*, *B. ferruginus*, *B. izecksohni*, *B. pernix* and *B. pombali* (Ribeiro *et al.* 2005; Alves *et al.* 2006; Ribeiro *et al.* 2017; Monteiro *et al.* 2018a), co-ossified with sphenethmoid in *B. albolineatus* and *B. coloratus* (Bornschein *et al.* 2016; Ribeiro *et al.* 2017); (5) squamosals robust with anterior zygomatic ramus long in *B. actaeus*, *B. albolineatus*, *B. brunneus*, *B. coloratus*, *B. curupira*, *B. ferruginus*, *B. izecksohni*, *B. pernix* and *B. pombali* (Ribeiro *et al.* 2005; Alves *et al.* 2006; Bornschein *et al.* 2016; Ribeiro *et al.* 2017; Monteiro *et al.* 2018a); (6) pterygoids relatively robust in *B. actaeus*, *B. albolineatus*, *B. brunneus*, *B. coloratus*, *B. curupira*, *B. ferruginus*, *B. izecksohni*, *B. pernix* and *B. pombali* (Ribeiro *et al.* 2005; Alves *et al.*

2006; Bornschein *et al.* 2016; Ribeiro *et al.* 2017; Monteiro *et al.* 2018a); (7) cultriform process of parasphenoid not fused to sphenethmoid in *B. actaeus*, *B. brunneus*, *B. coloratus*, *B. curupira*, *B. ferruginus*, *B. izecksohni*, *B. pernix* and *B. pombali* (Ribeiro *et al.* 2005; Alves *et al.* 2006; Ribeiro *et al.* 2017; Monteiro *et al.* 2018a), fused in *B. albolineatus* (Bornschein *et al.* 2016). Species of *B. didactylus* group have (Ribeiro *et al.* 2005; Alves *et al.* 2006; Condez *et al.* 2016): (1) absent neopalatines in *B. hermogenesi* and *B. sulfuratus*; (2) quadratojugals present in *B. hermogenesi* and *B. sulfuratus*; (3) maxillary odontoids present, numerous in *B. hermogenesi*; (4) vomers reduced in *B. hermogenesi*; (5) squamosals with anterior zygomatic ramus reduced and ramus ventral laterally expanded in *B. hermogenesi*; (6) pterygoids relatively robust *B. hermogenesi*; (7) cultriform process of parasphenoid not fused to sphenethmoid in *B. hermogenesi* or fused in *B. sulfuratus*. Species of *B. ephippium* group have: (1) absence of neopalatine in *B. bufonoides*, *B. crispus*, *B. darkside*, *B. guarani*, *B. toby* (Haddad *et al.* 2010; Clemente-Carvalho *et al.* 2012; Condez *et al.* 2014; Guimarães *et al.* 2017); (2) absence of quadratojugals in *B. bufonoides*, *B. darkside*, *B. ephippium*, *B. guarani*, *B. toby* (Campos *et al.* 2010; Haddad *et al.* 2010; Clemente-Carvalho *et al.* 2012; Guimarães *et al.* 2017), present in *B. crispus* (Condez *et al.* 2014); (3) maxillary odontoids absent in *B. bufonoides*, *B. crispus*, *B. darkside*, *B. guarani*, *B. toby* (Haddad *et al.* 2010; Clemente-Carvalho *et al.* 2012; Condez *et al.* 2014; Guimarães *et al.* 2017); (4) vomers reduced in *B. bufonoides*, *B. darkside* (Guimarães *et al.* 2017) and *B. ephippium* (Campos *et al.* 2010), fused in *B. crispus* and *B. guarani* (Clemente-Carvalho *et al.* 2012; Condez *et al.* 2014); (5) squamosals with zygomatic ramus short and ornamented in *B. bufonoides*, *B. crispus*, *B. darkside*, *B. ephippium*, *B. guarani* (Campos *et al.* 2010; Clemente-Carvalho *et al.* 2012; Condez *et al.* 2014; Guimarães *et al.* 2017); (6) fusion of the cultriform process of parasphenoid to sphenethmoid in *B. crispus* (Condez *et al.* 2014) and *B. bufonoides* and not fusion on *B. darkside*, and *B. ephippium* (Campos *et al.* 2010; Guimarães *et al.* 2017).

Regarding the appendicular osteology, *pes* of *B. actaeus*, *B. albolineatus*, *B. crispus*, *B. darkside*, *B. didactylus*, *B. ephippium*, *B. ferruginus*, *B. guarani*, *B. pombali*, and *B. toby* (Alberch and Gale 1985; Fabrezi 2001; Alves *et al.* 2006; Haddad *et al.* 2010; Clemente-Carvalho *et al.* 2012; Bornschein *et al.* 2016; Guimarães *et al.* 2017; Monteiro *et al.* 2018a) have one prehallical element as well as in the *B. bufonoides* described in the present study. On the other hand, *manus* has been described with two minutes elements for *B. actaeus* (Monteiro *et al.* 2018a), *B. ephippium* (Fabrezi 2001) as well as in *B. bufonoides*, however only one element seems to be present in prepollex of *B. albolineatus*, *B. crispus*, *B. darkside*, *B. ferruginus*, *B. guarani*, *B. pombali* and *B. toby* (see Alves *et al.* 2006; Haddad *et al.* 2010; Clemente-Carvalho *et al.* 2012; Condez *et al.* 2014; Bornschein *et al.* 2016; Guimarães *et al.* 2017). Moreover, the element *y* present on *manus* of *B. bufonoides*, as well as in *B. ephippium* (see Andersen 1978) and *B. albolineatus* (Bornschein *et al.* 2016), seems not to be present in *B. ferruginus* and *B. pombali* (see Alves *et al.* 2006).

Discussion

Brachycephalus bufonoides is distinguished from its congenics by morphological evidence, both internal and external, as well as bioacoustic and molecular traits. Although it has some overall external similarities with *B. crispus* and *B. vertebralis*, some characters such as the degree of hyperossification of the skull (very hyperossified in *B. bufonoides* and intermediate hyperossified in *B. crispus* and *B. vertebralis*) distinguishes among these species (Haddad *et al.* 2010; Condez *et al.* 2014). Furthermore, molecular data provide further evidence for its taxonomic status, being reciprocally monophyletic with its sister group.

Acoustic data has shown to be an important set of features to be used in species identification and delimitation (*e.g.*, Haddad and Pombal 1998; Canedo and Pombal 2007; Carvalho and Giaretta 2013), adding to our knowledge of these taxa, as the advertisement call is a vital part of the anurans' life history. Acoustically, *Brachycephalus bufonoides* differs from its congenics mostly by temporal aspects of its advertisement call, such as note duration, number of pulses per note and repetition rate. *Brachycephalus bufonoides* appears to be the only species in the genus that presents a strong pulse-period modulation throughout the call, though further investigation must be done in order to assert this character state in other species. Harmonics have only been detected in call belonging to *B. darkside* (Guimarães *et al.* 2017).

Absence of bones such as the neopalatine and columellae in the skull, phalangeal loss and a reduced number of toes are believed to have evolved by miniaturization (Yeh 2002; Clemente-Carvalho *et al.* 2011). The skull's curvature is noteworthy, more evident in miniaturized frogs (Yeh 2002), and present in the skull of *Brachycephalus*. Another osteological phenotypic feature among the species of *Brachycephalus* is a gradient in the degree of miner-

alization of the skeleton, which is remarkable with the presence of hyperossified skull and the spinal processes of sacral and presacral vertebrae are hyperossified, or of a dorsal shield in *B. ephippium* group (Clemente-Carvalho *et al.* 2009; Clemente-Carvalho *et al.* 2012).

Studies involving *Brachycephalus* osteology usually do not include hyolaryngeal descriptions (except Trewavas 1933; Ribeiro *et al.* 2005; Alves *et al.* 2006; Ribeiro *et al.* 2017). Trewavas (1933) completely describe the hyolaryngeal apparatus but not figured it. Other species of *Brachycephalus* had the hyolaryngeal structures restricted to some comments throughout the osteological descriptions, as the shape of posteromedial processes of the hyoid and mineralized arytenoid cartilages of *B. coloratus* (Ribeiro *et al.* 2017). Thereby, laryngeal structures are pictured for the first time in the present work. We also give a full description of the hyolaryngeal structures.

Brachycephalus bufonoides belongs to the *B. ephippium* species group and to *B. vertebralis* lineage. This species is sister of a clade composed of *B. alipioi* (*(B. vertebralis + B. pitanga) (B. toby + B. nodoterga)*). A similar relationship was recovered by Condez *et al.* (2020), being *B. alipioi* the second species to diverge (*B. sp. 2* was the first one) within *B. vertebralis* lineage. *Brachycephalus vertebralis* and *B. pitanga* but nested with *B. crispus*, *B. sp. 3* and *B. guarani*. This clade was the sister group of *Brachycephalus nodoterga + B. toby*. Ribeiro *et al.* (2015) recognized three species groups within *Brachycephalus*, *B. ephippium* group (known in southeastern Brazil), *B. pernix* group (known in south Brazil), and *B. didactylus* (with wider distribution). *Brachycephalus didactylus* group was not recovered as a monophyletic group, as well as other studies so far (Clemente-Carvalho *et al.* 2011; Condez *et al.* 2016; Monteiro *et al.* 2018a; Condez *et al.* 2020). We are aware that for a robust relationship proposal among *Brachycephalus* species, a broader study including more genes (here only 16S was used) and morphological data is needed, however, with the available evidence so far, *B. didactylus* group should not be used.

The mountain range near the metropolitan region of Rio de Janeiro, southeastern Brazil, including the type locality of *Brachycephalus bufonoides*, shows high endemism and richness of anurans. There, recently, anuran species were found in nature for the first time (*Hylodes pipilans*: Canedo and Pombal 2007; *Holoaden pholeter*: Pombal *et al.* 2008; *Cycloramphus organensis*: Weber *et al.* 2008; *Fritziana izecksohni*: Folly *et al.* 2018) or rediscovered (*F. ulei*: Folly *et al.* 2014). The rediscovery of *Brachycephalus bufonoides* reiterates the importance of this region for the conservation of the Atlantic Forest biodiversity, one of the highest in anuran species richness worldwide (Duellman 1999).

Apparently, *Brachycephalus bufonoides* is among those which the geographic distribution is extremely restricted; evidencing how high altitude may contribute to a high degree of endemism. Ranges of specific climatic zones, geographic barriers and diversity of habitats found on mountains create ideal conditions for species isolation (Spehn *et al.* 2010; Merckx *et al.* 2015). As mountaintops function as islands, species isolation and speciation play a huge role in high-elevation biodiversity following patterns similar to insular isolation (Brown 1978). Of the 36 known species of the genus, of the 22 described the last ten years, 14 are only known from their type locality (Frost 2019; Bornschein *et al.* 2019a; present study), which consists mostly of high-elevation areas (Pie *et al.* 2013), while species such as *B. didactylus* and *B. sulfuratus*, with broader distribution usually inhabit the lowlands (Condez *et al.* 2016; Pie *et al.* 2013). However, in most cases, species of *Brachycephalus* are locally abundant, their restricted distributions and range sizes, along with the fact that most of them constitute high-elevation species, makes them naturally more vulnerable when we consider factors such as habitat loss, fragmentation, and climate change (*e.g.*, McDonald and Brown 1992; Pounds *et al.* 2006; Dirnböck *et al.* 2011).

Finally, herein an important contribution for the taxonomy and systematics of this genus is provided, including a large amount of novel information for *B. bufonoides* from different sources (*i.e.*, molecular, morphological variation, bioacoustic), allowing it to be included in future studies of species delimitation and relationships within *Brachycephalus*.

Acknowledgments

We are thankful to the Ministério do Meio Ambiente (SISBIO 23501-1/2010) for the collecting permits. We are indebted to C.F.B Haddad, T. Grant, and F. Toledo for allowing access to the specimens under their care, V. Urzua for allowing access to the study area, and L. Veiga for assistance during the fieldwork. We are also indebted to S. Ferreira who did the tomography of the species very quickly and with T. Grant that provided the performing of the tomography. S.G. Pinheiro and G.A. Pinheiro for logistic support in fieldwork; M.W. Cardoso for helpful with the

osteology description; L. Barreto made the drawings ink. We thank C.F.B. Haddad, R. Sawaya and C. de Luna-Dias for providing unpublished photos of species of *Brachycephalus* in life. A. Benetti, J. Botero, R. Sousa, and V. Urso-Guimarães assistance in laboratory work. We also are thankful to C.R. Hutter for reviewing the manuscript. The authors thank the reviewer T.H. Condez and J.P.C. Monteiro for providing valuable suggestions on the manuscript. MF was supported by a postdoctoral fellowship from Conselho Nacional de Desenvolvimento Científico e Tecnológico (CNPq) (154743/2018-6); SPCS is grateful by grant from CNPq; JPP was supported by grants from CNPq and Faperj.

References

- Alberch, P. & Gale, E.A. (1985) A developmental analysis of an evolutionary trend: digital reduction in amphibians. *Evolution*, 39, 8–23.
<https://doi.org/10.1111/j.1558-5646.1985.tb04076.x>
- Almeida-Santos, M. Siqueira, C.C., Van Sluys, M. & Rocha, C.F.D. (2011) Ecology of the Brazilian flea frog *Brachycephalus didactylus* (Terrarana: Brachycephalidae). *Journal of Herpetology*, 45 (2), 251–255.
<https://doi.org/10.1670/10-015.1>
- Altschul, S.F., Madden, T.L., Schäffer, A.A., Zhang, J., Zhang, Z., Miller, W. & Lipman, D.J. (1997) Gapped BLAST and PSI-BLAST: a new generation of protein database search programs. *Nucleic Acids Research*, 25 (17), 3389–3402.
<https://doi.org/10.1093/nar/25.17.3389>
- Alves, A.C.R., Ribeiro, L.F., Haddad, C.F.B. & Reis, S.F. (2006) Two new species of *Brachycephalus* (Anura: Brachycephalidae) from the Atlantic forest in Paraná State, southern Brazil. *Herpetologica*, 62 (2), 221–233.
<https://doi.org/10.1655/05-41.1>
- Alves, A.C.R., Sawaya, R., Reis, S.F. & Haddad, C.B.F. (2009) A new species of *Brachycephalus* (Anura: Brachycephalidae) from the Atlantic Rain Forest in São Paulo State, Southeastern Brazil. *Journal of Herpetology*, 43 (2), 212–219.
<https://doi.org/10.1670/0022-1511-43.2.212>
- Andersen, M.L. (1978) *The comparative myology and osteology of the carpus and tarsus of selected anurans*. Ph.D. dissertation, University of Kansas, Lawrence, Kansas, 295 pp.
- Angulo, A. & Reichle, S. (2008) Acoustic signals, species diagnosis, and species concepts: the case of a new cryptic species of *Leptodactylus* (Amphibia, Anura, Leptodactylidae) from the Chapare region, Bolivia. *Zoological Journal of the Linnean Society*, 152 (1), 59–77.
<https://doi.org/10.1111/j.1096-3642.2007.00338.x>
- Araújo, C.B., Guerra, T.J., Amatuzzi, M.C.O. & Campos, L.A. (2012) Advertisement and territorial calls of *Brachycephalus pitanga* (Anura: Brachycephalidae). *Zootaxa*, 3302 (1), 66–67.
<https://doi.org/10.11646/zootaxa.3302.1.5>
- Bokermann, W.C.A. (1966) *Lista anotada das localidades tipo de anfíbios brasileiros*. Serviço de Documentação, São Paulo, 183 pp.
- Bornschein, M.R., Ribeiro, L.F., Blackburn, D.C., Stanley, E.L. & Pie, M.R. (2016) A new species of *Brachycephalus* (Anura: Brachycephalidae) from Santa Catarina, southern Brazil. *PeerJ*, 4 (e2629), 1–19.
<https://doi.org/10.7717/peerj.2629>
- Bornschein, M.R., Ribeiro, L.F., Rollo Jr., M.M., Confetti, A.E. & Pie, M.R. (2017) Advertisement call of *Brachycephalus albolineatus* (Anura: Brachycephalidae). *PeerJ*, 6 (e5273), 1–18.
<https://doi.org/10.7287/peerj.preprints.3461v1>
- Bornschein, M.R., Pie, M.R. & Teixeira, L. (2019a) Conservation Status of *Brachycephalus* Toadlets (Anura: Brachycephalidae) from the Brazilian Atlantic Rainforest. *Diversity*, 11, 150, 1–29.
<https://doi.org/10.3390/d11090150>
- Bornschein, M.R., Rollo, M.M., Pie, M.R., Confetti, A.E. & Ribeiro, L.F. (2019b) Redescription of the advertisement call of *Brachycephalus tridactylus* (Anura: Brachycephalidae). *Phyllomedusa*, 18 (1), 3–12.
<https://doi.org/10.11606/issn.2316-9079.v18i1p3-12>
- Brown, J.H. (1978) The theory of insular biogeography and the distribution of boreal birds and mammals. *Great Basin Naturalist Memoirs*, 2, 209–227.
- Campos, L.A., Silva, H.R. & Sebben, A. (2010) Morphology and development of additional bony elements in the genus *Brachycephalus* (Anura: Brachycephalidae). *The Biological Journal of the Linnean Society*, 99 (4), 752–767.
<https://doi.org/10.1111/j.1095-8312.2010.01375.x>
- Canedo, C. & Pombal, J.P. Jr. (2007) Two new species of torrent frog of the genus *Hylodes* (Anura, Hylodidae) with nuptial thumb tubercles. *Herpetologica*, 63 (2), 224–235.
[https://doi.org/10.1655/0018-0831\(2007\)63\[224:TNSOTF\]2.0.CO;2](https://doi.org/10.1655/0018-0831(2007)63[224:TNSOTF]2.0.CO;2)
- Carvalho, T.R. & Giaretta, A.A. (2013) Taxonomic circumscription of *Adenomera martinezi* (Bokermann, 1956) (Anura: Leptodactylidae: Leptodactylinae) with the recognition of a new cryptic taxon through a bioacoustic approach. *Zootaxa*, 3701 (2), 207–237.

<https://doi.org/10.11646/zootaxa.3701.2.5>

- Cei, J.M. (1980) *Amphibians of Argentina. Monitore Zoologico Italiano. New Series. Monograph 2*. Instituto de Biologia Animal, Facultad de Ciencias Agrarias, Universidad Nacional de Cuyo, Mendoza, 609 pp.
- Clemente-Carvalho, R.B., Antoniazzi, M.M., Jared, C., Haddad, C.F., Alves, A.C., Rocha, H.S., Pereira, G.R., Oliveira, D.F., Lopes, R.T. & dos Reis, S.F. (2009) Hyperossification in miniaturized toadlets of the genus *Brachycephalus* (Amphibia: Anura: Brachycephalidae): microscopic structure and macroscopic patterns of variation. *Journal of Morphology*, 270 (11), 1285–1295.
<https://doi.org/10.1002/jmor.10755>
- Clemente-Carvalho, R.B.G., Klaczko, J., Perez, S.I., Alves, A.C.R., Haddad, C.F.B. & dos Reis, S.F. (2011) Molecular phylogenetic relationships and phenotypic diversity in miniaturized toadlets, genus *Brachycephalus* (Amphibia: Anura: Brachycephalidae). *Molecular Phylogenetics and Evolution*, 61 (1), 79–89.
<https://doi.org/10.1016/j.ympev.2011.05.017>
- Clemente-Carvalho, R.B.G., Giaretta, A.A., Condez, T.H., Haddad, C.F.B. & dos Reis, S.F. (2012) A new species of miniaturized toadlet, genus *Brachycephalus* (Anura: Brachycephalidae), from the Atlantic forest of Southeastern Brazil. *Herpetologica*, 68 (3), 365–374.
<https://doi.org/10.1655/HERPETOLOGICA-D-11-00085.1>
- Cochran, D.M. (1955) Frogs of southeastern Brazil. *Bulletin of the United States National Museum*, 206, 1–423.
<https://doi.org/10.5479/si.03629236.206.1>
- Condez, T.H., Clemente-Carvalho, R.B.G., Haddad, C.F.B. & dos Reis, S.F. (2014) A new species of *Brachycephalus* (Anura: Brachycephalidae) from the highlands of the Atlantic Forest, Southeastern Brazil. *Herpetologica*, 70 (1), 89–99.
<https://doi.org/10.1655/HERPETOLOGICA-D-13-00044>
- Condez, T.H., Monteiro, J.P.C., Comitti, E.J., Garcia, P.C.A., Amaral, I.B. & Haddad, C.F.B. (2016) A new species of flea-toad (Anura: Brachycephalidae) from southern Atlantic Forest, Brazil. *Zootaxa*, 4083 (1), 40–56.
<https://doi.org/10.11646/zootaxa.4083.1.2>
- Condez, T.H., Haddad, C.F.B. & Zamudio, K.R. (2020) Historical biogeography and multi-trait evolution in miniature toadlets of the genus *Brachycephalus* (Anura: Brachycephalidae), *Biological Journal of the Linnean Society*, 129 (3), 664–686.
<https://doi.org/10.1093/biolinnean/blz200>
- Dirnböck, T., Essl, F. & Rabitsch, W. (2011) Disproportional risk for habitat loss of high-altitude endemic species under climate change. *Global Change Biology*, 17 (2), 990–996.
<https://doi.org/10.1111/j.1365-2486.2010.02266.x>
- Dorigo, T.A., Siqueira, C.C., Vrcibradic, D., Maia-Carneiro, T., Almeida-Santos, M. & Rocha, C.F.D. (2012) Ecological aspects of the pumpkin toadlet, *Brachycephalus garbeanus* Miranda-Ribeiro, 1920 (Anura: Neobatrachia: Brachycephalidae), in a highland forest of southeastern Brazil. *Journal of Natural History*, 46 (39–40), 2497–2507. <https://doi.org/10.1080/00222933.2012.713525>
- Duellman, W.E. (1970) *The hylids frogs of Middle America*. Monograph of the Museum of Natural History, University of Kansas, Lawrence, Kansas, pp.
- Duellman, W.E. (1999) Global distribution of amphibians: patterns, conservation, and future challenges. In: Duellman, W.E. (Ed.), *Patterns of distribution of amphibians: a global perspective*. Johns Hopkins University Press, Baltimore, Maryland, pp. 1–30
- Fabrezi, M. (1992) El carpo de los anuros. *Alytes*, 10, 1–36.
- Fabrezi, M. (1993) The anuran tarsus. *Alytes*, 11, 47–63.
- Fabrezi, M. (2001) A survey of prepollex and prehallux variation in anuran limbs. *Zoological Journal of the Linnean Society*, 131 (2), 227–248.
<https://doi.org/10.1111/j.1096-3642.2001.tb01316.x>
- Felsenstein, J. (1985) Confidence limits on phylogenies, an approach using bootstrap. *Evolution*, 39 (4), 783–791.
<https://doi.org/10.1111/j.1558-5646.1985.tb00420.x>
- Firkowski, C.R., Bornschein, M.R., Ribeiro, L.F. & Pie, M.R. (2016) Species delimitation, phylogeny and evolutionary demography of co-distributed, montane frogs in the southern Brazilian Atlantic Forest. *Molecular Phylogenetics and Evolution*, 100, 345–360.
<https://doi.org/10.1016/j.ympev.2016.04.023>
- Folly, M., Hepp, F., Carvalho-e-Silva, S.P. & Duellman, W.E. (2014) Taxonomic status and redescription of *Flectonotus ulei* (Anura: Hemiphractidae), with a key for the species of *Fritziana*. *Zoologia*, 31 (4), 393–399. <https://doi.org/10.1590/S1984-46702014000400011>
- Folly, M., Hepp, F. & Carvalho-e-Silva, S.P. (2018) A new bromeligenous species of *Fritziana* Mello-Leitão, 1937 (Amphibia: Anura: Hemiphractidae) from high elevations in the Serra dos Órgãos, Rio de Janeiro, Brazil. *Herpetologica*, 74 (1), 58–72.
<https://doi.org/10.1655/Herpetologica-D-16-00035>
- Frost, D.R. (2019) Amphibian Species of the World: An Online Reference. American Museum of Natural History, New York, USA. 21 May 2019. Available from: <http://research.amnh.org/herpetology/amphibia/index.html> (accessed 21 December 2019)
- Garey, M.V., Lima, A.M.X., Hartmann, M.T. & Haddad, C.F.B. (2012) A new species of miniaturized toadlet, genus *Brachy-*

- cephalus* (Anura: Brachycephalidae), from southern Brazil. *Herpetologica*, 68 (2), 266–271.
<https://doi.org/10.1655/HERPETOLOGICA-D-11-00074.1>
- Giaretta, A.A. & Sawaya, R.J. (1998) Second species of *Psyllophryne* (Anura: Brachycephalidae). *Copeia*, 1998 (4), 985–987.
<https://doi.org/10.2307/1447345>
- Goloboff, P.A., Farris, J.S. & Nixon, K.C. (2003) T.N.T.: Tree analysis using new technology. Program and documentation. Available from: <http://www.zmuc.dk/public/phylogeny> (accessed 21 December 2019)
- Goutte, S., Mason, M.J., Christensen-Dalsgaard, J., Montealegre-Z, F., Chivers, B.D., Sarria-S, F.A., Antoniazzi, M.M., Jared, C., Sato, L.A. & Toledo, L.F. (2017) Evidence of auditory insensitivity to vocalization frequencies in two frogs. *Scientific Reports*, 7 (12121), 1–9.
<https://doi.org/10.1038/s41598-017-12145-5>
- Guimarães, C. da S., Luz, S., Rocha, P.C. & Feio, R.N. (2017) The dark side of pumpkin toadlet: a new species of *Brachycephalus* (Anura: Brachycephalidae) from Serra do Brigadeiro, southeastern Brazil. *Zootaxa*, 4258 (4), 327–344.
<https://doi.org/10.11646/zootaxa.4258.4.2>
- Haddad, C.F.B., Alves, A.C.R., Clemente-Carvalho, R.B.G. & dos Reis, S.F. (2010) A new species of *Brachycephalus* from the Atlantic Rain Forest in São Paulo State, southeastern Brazil (Amphibia: Anura: Brachycephalidae). *Copeia*, 2010 (3), 410–420.
<https://doi.org/10.1643/CH-09-102>
- Haddad, C.F.B. & Pombal, J.P. Jr. (1998) Redescription of *Physalaemus spiniger* (Anura: Leptodactylidae) and description of two new reproductive modes. *Journal of Herpetology*, 32 (4), 557–565.
<https://doi.org/10.2307/1565210>
- Hedges, S.B., Duellman, W.E. & Heinicke, M.P. (2008) New World direct-development frogs (Anura: Terrarana): Molecular phylogeny, classification, biogeography, and conservation. *Zootaxa*, 1737 (1), 1–182.
<https://doi.org/10.11646/zootaxa.1737.1.1>
- Hedges, S.B. (1994) Molecular evidence for the origin of birds. *Proceedings of the National Academy of Sciences of the United States of America*, 91 (7), 2621–2624.
<https://doi.org/10.1073/pnas.91.7.2621>
- Heyer, W.R., Rand, A.S. Cruz, C.A.G., Peixoto, O.L. & Nelson, C.E. (1990) Frogs of Boracéia. *Arquivos de Zoologia*, 31, 231–410.
- Hepp, F. & Pombal, J.P. Jr. (2019) Naming structures and qualifying properties of anuran bioacoustical signals: a call for homology-based nomenclature and equality for quantitative data. *Anais da Academia Brasileira de Ciências*, 91 (4), e20190965.
<https://doi.org/10.1590/0001-3765201920190965>
- Ihering, H.V. & Ihering, R.V. (1911) O Museu Paulista nos anos de 1906 a 1909. *Revista do Museu Paulista*, 8, 1–22.
<https://doi.org/10.5962/bhl.part.20998>
- Instituto Brasileiro de Geografia e Estatística—IBGE (1959) *Enciclopédia dos municípios brasileiros*. IBGE, Rio de Janeiro, 467 pp.
- Izecksohn, E. (1971) Novo gênero e nova espécie de Brachycephalidae do Estado do Rio de Janeiro, Brasil (Amphibia, Anura). *Boletim do Museu Nacional*, Boletim do Museu Nacional (N.S.), Zoologia, New Series, Zoologia, 280, 1–12.
- Katoh, K. & Standley, D.M. (2013) MAFFT multiple sequence alignment software version 7: improvements in performance and usability. *Molecular Biology and Evolution*, 30 (4), 772–780.
<https://doi.org/10.1093/molbev/mst010>
- Kearse, M., Moir, R., Wilson, A., Stones-Havas, S., Cheung, M., Sturrock, S., Buxton, S., Cooper, A., Markowitz, S., Duran, C., Thierer, T., Ashton, B., Meintjes, P. & Drummond, A. (2012) Geneious Basic: an integrated and extendable desktop software platform for the organization and analysis of sequence data. *Bioinformatics*, 28 (12), 1647–1649.
<https://doi.org/10.1093/bioinformatics/bts199>
- Köhler, J., Jansen, M., Rodrigues, A., Kok, P.J.R., Toledo, L.F., Emmrich, M., Glaw, F., Haddad, C.F.B., Rödel, M.O. & Vences, M. (2017) The use of bioacoustics in anuran taxonomy: theory, terminology, methods and recommendations form best practice. *Zootaxa*, 4251 (1), 1–124.
<https://doi.org/10.11646/zootaxa.4251.1.1>
- Koichiro, T., Stecher, G., Peterson, D., Filipowski, A. & Kumar, S. (2013) MEGA6: Molecular Evolutionary Genetics Analysis version 6.0. *Molecular Biology and Evolution*, 30 (12), 2725–2729.
<https://doi.org/10.1093/molbev/mst197>
- Littlejohn, M.J. (2001) Patterns of differentiation in temporal properties of acoustic signals of anurans. In: Ryan, M.J. (Ed.), *Anuran Communication*. Smithsonian Institution Press, Washington, pp. 102–120.
- McDonald, K. & Brown, J.H. (1992) Using montane mammals to model extinctions due to global change. *Conservation Biology*, 6 (3), 409–415.
<https://doi.org/10.1046/j.1523-1739.1992.06030409.x>
- Merckx, V.S.F.T., Hendriks, K.P., Beentjes, K.K., Mennes, C.B., Becking, L.E., Peijnenburg, K.T.C.A., Afendy, A., Arumugam, N., de Boer, H., Biun, A., Buang, M.M., Chen, P., Chung, A.Y.C., Dow, R., Feijen, F.A.A., Feijen, H., Soest, C.F., Geml, J., Geurts, R., Gravendeel, B., Hovenkamp, P., Imbun, P., Ipor, I., Janssens, S.B., Jocqué, M., Kappes, H., Khoo, E., Koomen, P., Lens, F., Majapun, R.J., Morgado, L.N., Neupane, S., Nieser, N., Pereira, J.T., Rahman, H., Sabran, S., Sawang, A., Schwallier, R.M., Shim, P., Smit, H., Sol, N., Spait, M., Stech, M., Stokvis, F., Sugau, J.B., Suleiman, M., Sumail, S.,

- Thomas, D.C., van Tol, J., Tuh, F.Y.Y., Yahya, B.E., Nais, J., Repin, R., Lakim, M. & Schilthuizen, M. (2015) Evolution of endemism on a young tropical mountain. *Nature*, 524, 347–350.
<https://doi.org/10.1038/nature14949>
- Miranda-Ribeiro, A. (1920) Os Brachycephalideos do Museu Paulista (com três especies novas). *Revista do Museu Paulista*, 12, 307–316.
<https://doi.org/10.5962/bhl.part.22255>
- Monteiro, J.P.C., Condez, T.H., Garcia, P.C.A., Comitti, E.J., Amaral, I.B. & Haddad, C.F.B. (2018a) A new species of *Brachycephalus* (Anura, Brachycephalidae) from the coast of Santa Catarina State, southern Atlantic Forest, Brazil. *Zootaxa*, 4407 (4), 483–505.
<https://doi.org/10.11646/zootaxa.4407.4.2>
- Monteiro, J.P.C., Condez, T.H., Garcia, P.C.A. & Haddad, C.F.B. (2018b) The advertisement calls of two species of *Brachycephalus* (Anura: Brachycephalidae) from southern forest Brazil. *Zootaxa*, 4415 (1), 183–188.
<https://doi.org/10.11646/zootaxa.4415.1.10>
- Napoli, M.F., Caramaschi, U., Cruz, C.A.G. & Dias, I.R. (2011) A new species of flea-toad, genus *Brachycephalus* Fitzinger (Amphibia: Anura: Brachycephalidae), from the Atlantic rainforest of southern Bahia, Brazil. *Zootaxa*, 2739 (1), 33–40.
<https://doi.org/10.11646/zootaxa.2739.1.3>
- Oliveira, E.G. & Haddad, C.F.B. (2015) Diet Seasonality and Feeding Preferences of *Brachycephalus pitanga* (Anura: Brachycephalidae). *Journal of Herpetology*, 49 (2), 252–256.
<https://doi.org/10.1670/13-211>
- Padial, J.M., Grant, T. & Frost, D.R. (2014) Molecular systematics of terraranas (Anura: Brachycephaloidea) with an assessment of the effects of alignment and optimality criteria. *Zootaxa*, 3825 (1), 1–132.
<https://doi.org/10.11646/zootaxa.3825.1.1>
- Palumbi, S.R., Martin, A., McMillan, W.O., Stice, L. & Grabowski, G. (1991) *The simple fool's guide to PCR*. Version 2.0. Privately published, compiled by Palumbi S., Department of Zoology, University of Hawaii, Honolulu, 47 pp.
- Pie, M.R., Meyer, A.L.S., Firkowski, C.R., Ribeiro, L.F. & Bornschein, M.R. (2013) Understanding the mechanisms underlying the distribution of microendemic montane frogs (*Brachycephalus* spp., Terrarana: Brachycephalidae) in the Brazilian Atlantic Rainforest. *Ecological Modelling*, 250, 165–176.
<https://doi.org/10.1016/j.ecolmodel.2012.10.019>
- Pie, M.R. & Ribeiro, L.F. (2015) A new species of *Brachycephalus* (Anura: Brachycephalidae) from the Quiriri mountain range of southern Brazil. *PeerJ*, 3 (e1179), 1–9.
<https://doi.org/10.7717/peerj.1179>
- Pie, M.R., Ribeiro, L.F., Confetti, A.E., Nadaline, M.J. & Bornschein, M.R. (2018) A new species of *Brachycephalus* (Anura: Brachycephalidae) from southern Brazil. *PeerJ*, 6 (e5683), 1–27.
<https://doi.org/10.7717/peerj.5683>
- Pombal, J.P. Jr. (1999) Oviposição e desenvolvimento de *Brachycephalus ephippium* (Spix) (Anura: Brachycephalidae). *Revista Brasileira de Zoologia*, 16 (4), 947–956.
<https://doi.org/10.1590/S0101-81751999000400004>
- Pombal, J.P. Jr. (2010) A posição taxonômica das variedades de *Brachycephalus ephippium* (Spix, 1824) descritas por Miranda-Ribeiro, 1920 (Amphibia, Anura, Brachycephalidae). *Boletim do Museu Nacional (N.S.), Zoologia*, 526, 1–12.
- Pombal, J.P. Jr. & Gasparini, J.L. (2006) A new *Brachycephalus* (Anura: Brachycephalidae) from the Atlantic Rainforest of Espírito Santo, southeastern Brazil. *South American Journal of Herpetology*, 1 (2), 87–93.
[https://doi.org/10.2994/1808-9798\(2006\)1\[87:ANBABF\]2.0.CO;2](https://doi.org/10.2994/1808-9798(2006)1[87:ANBABF]2.0.CO;2)
- Pombal, J.P. Jr. & Izecksohn, E. (2011) Uma nova espécie de *Brachycephalus* (Anura: Brachycephalidae) do estado do Rio de Janeiro. *Papéis Avulsos de Zoologia*, 51 (28), 443–451.
<https://doi.org/10.1590/S0031-10492011002800001>
- Pombal, J.P. Jr., Sazima, I. & Haddad, C.F.B. (1994) Breeding behavior of the pumpkin toadlet, *Brachycephalus ephippium* (Brachycephalidae). *Journal of Herpetology*, 28 (4), 516–519.
<https://doi.org/10.2307/1564972>
- Pombal, J.P. Jr., Wistuba, E.M. & Bornschein, M.R. (1998) A new species of brachycephalid (Anura) from the Atlantic Rain Forest of Brazil. *Journal of Herpetology*, 32 (1), 70–74.
<https://doi.org/10.2307/1565481>
- Pombal, J.P. Jr., Siqueira, C.C., Dorigo, T.A., Vrcibradic, D. & Rocha, C.F.D. (2008) A third species of the rare frog genus *Holoaden* (Terrarana, Strabomantidae) from a montane rainforest area of southeastern Brazil. *Zootaxa*, 1938 (1), 61–68.
<https://doi.org/10.11646/zootaxa.1938.1.4>
- Posada, D. (2008) jModelTest: Phylogenetic Model Averaging. *Molecular Biology and Evolution*, 25 (7), 1253–1256.
<https://doi.org/10.1093/molbev/msn083>
- Pounds, J.A., Bustamante, M.R., Coloma, L.A., Consuegra, J.A., Fodgen, M.P.L., Foster, P.N., La Marca, E., Masters, K.L., Merino-Viteri, A., Puschendorf, R., Ron, S.R., Sánchez-Azofeifa, G.A., Still, C.J. & Young, B.E. (2006) Widespread amphibian extinctions from epidemic disease driven by global warming. *Nature*, 439, 161–167.
<https://doi.org/10.1038/nature04246>
- Pugener, L.A. & Maglia, A.M. (1997) Osteology and skeletal development of *Discoglossus sardus* (Anura: Discoglossidae).

- Journal of Morphology*, 233 (3), 267–286.
[https://doi.org/10.1002/\(SICI\)1097-4687\(199709\)233:3<267::AID-JMOR6>3.0.CO;2-0](https://doi.org/10.1002/(SICI)1097-4687(199709)233:3<267::AID-JMOR6>3.0.CO;2-0)
- R Core Team R (2016) R: A language and environment for statistical computing. R Foundation for Statistical Computing, Vienna, Austria. Available from: <http://www.r-project.org/> (accessed 24 December 2019)
- Rambaut, A. & Drummond, A. (2007) TRACER. MCMC trace analysis tool. Version 1.4. University of Oxford, Oxford. Available from: <http://tree.bio.ed.ac.uk/software/tracer> (accessed 24 December 2019)
- Ribeiro, L.F., Alves, A.C.R., Haddad, C.F.B. & Reis, S.F. dos (2005) Two new species of *Brachycephalus* Günther, 1858 from the State of Paraná, southern Brazil (Amphibia, Anura, Brachycephalidae). *Boletim do Museu Nacional, New Series, Zoologia*, 519, 1–18.
- Ribeiro, L.F., Bornschein, M.R., Belmonte-Lopes, R., Firkowski, C.R., Morato, S.A.A. & Pie, M.R. (2015) Seven new micro-endemic species of *Brachycephalus* (Anura: Brachycephalidae) from southern Brazil. *PeerJ*, 3, e1011.
<https://doi.org/10.7717/peerj.1011>
- Ribeiro, L.F., Blackburn, D.C., Stanley, E.L., Pie, M.R. & Bornschein, M.R. (2017) Two new species of the *Brachycephalus pernix* group (Anura: Brachycephalidae) from the state of Paraná, southern Brazil. *PeerJ*, 5, e3603.
<https://doi.org/10.7717/peerj.3603>
- Ronquist, F., Teslenko, M., Mark, P. van der, Ayres, D.L., Darling, A., Höhna, S., Larget, B., Liu, L., Suchard, M.A. & Huelsenbeck, J.P. (2012) MRBAYES 3.2: Efficient Bayesian phylogenetic inference and model selection across a large model space. *Systematic Biology*, 61 (3), 539–542.
<https://doi.org/10.1093/sysbio/sys029>
- Sabaj, M.H. (2016) Standard symbolic codes for institutional resource collections in herpetology and ichthyology: an online reference. Version 6.5. American Society of Ichthyologists and Herpetologists, Washington, D.C. Available from: <http://www.asih.org/> (accessed 16 August 2016)
- Siqueira, C.C., Vrcibradic, D., Nogueira-Costa, P., Martins, A.R., Dantas, L., Gomes, V.L.R., Bergallo, H.G. & Rocha, C.F.D. (2014) Environmental parameters affecting the structure of leaf-litter frog (Amphibia: Anura) communities in tropical forests: a case study from an Atlantic Rainforest area in Southeastern Brazil. *Iheringia, Zoologia*, 31 (2), 147–152.
<https://doi.org/10.1590/S1984-46702014000200005>
- Spehn, E.M., Rudmann-Maurer, K., Körner, C. & Maselli, D. (2010) *Mountain biodiversity and global change*. GMBM-DI-VERSITAS, University of Basel, Basel, 59 pp.
- Tandel, M.C.F.F., Loibel, S., Oliveira, E.G. & Haddad, C.F.B. (2014) Diferenciação de 3 tipos de vocalizações (cantos) na espécie *Brachycephalus pitanga*. *Revista da Estatística da Universidade Federal de Ouro Preto*, 3, 374–386.
- Taylor, W.R. & Van Dyke, G.C. (1985) Revised procedures for staining and clearing small fishes and other vertebrates for bone and cartilage study. *Cybiurn*, 9, 107–119.
- Trewavas, E. (1933) The hyoid and larynx of the Anura. *Philosophical transactions of the Royal Society of London, Series B*, 222, 410–527.
<https://doi.org/10.1098/rstb.1932.0020>
- Trueb, L. (1973) Bones, frogs, and evolution. In: Vial, J.L. (Ed.), *Evolutionary biology of anurans: contemporary research on major problems*. University of Missouri Press, Columbia, Missouri, pp. 65–132.
- Trueb, L. (2015) Osteology. In: Duellman, W.E. (Ed.), *Marsupial frog: Gastrotheca and allied genera*. Johns Hopkins University Press, Baltimore, Maryland, pp. 31–51.
- Verdade, V.K., Rodrigues, M.T., Cassimiro, J., Pavan, D., Liou, N. & Lange, M.C. (2008) Advertisement call, vocal activity, and geographic distribution of *Brachycephalus hermogenesi* (Giaretta and Sawaya, 1998) (Anura: Brachycephalidae). *Journal of Herpetology*, 42 (3), 542–549.
<https://doi.org/10.1670/07-287.1>
- Weber, L.N., Verdade, V.K., Salles, R.O.L., Fouquet, A. & Carvalho-e-Silva, S.P. de (2008) A new species of *Cycloramphus* Tschudi (Anura: Cycloramphidae) from the Parque Nacional da Serra dos Órgãos, southeastern Brazil. *Zootaxa*, 2737 (1), 19–33.
<https://doi.org/10.11646/zootaxa.2737.1.2>
- Wilkinson, J.A., Matsui, M. & Terachi, T. (1996) Geographic variation in a Japanese tree frog (*Rhacophorus arboreus*) revealed by PCR-aided restriction site analysis of mtDNA. *Journal of Herpetology*, 30 (3), 418–423.
<https://doi.org/10.2307/1565184>
- Wistuba, E.M. (1998) *História natural de Brachycephalus pernix Pombal, Wistuba and Bornschein, 1998 (Anura) no Morro Anhangava, Município de Quatro Barras, Estado do Paraná*. M.Sc. dissertation, Universidade Federal do Paraná, Curitiba, 89 pp.
- Yeh, J. (2002) The effect of miniaturized body size on skeletal morphology in frogs. *Evolution*, 56 (3), 628–641.
<https://doi.org/10.1111/j.0014-3820.2002.tb01372.x>
- Zeileis, A. & Grothendieck, G. (2005) Zoo: s3 Infrastructure for Regular and Irregular Time Series. *Journal of Statistical Software*, 14 (6), 1–7.
<https://doi.org/10.18637/jss.v014.i06>

APPENDIX I. Additional specimens examined from Brazil.

- Brachycephalus albolineatus*: state of SANTA CATARINA: Morro da Boa Vista, border between the municipalities of Jaraguá do Sul, and Massaranduba MNRJ 90349 (paratype).
- Brachycephalus alipioi*: state of ESPÍRITO SANTO: municipality of *Santa Teresa* MNRJ 25405–07; municipality of *Vargem Alta*, Fazenda Aoki CFBH 3566–67 (paratypes), MNRJ 26042 (holotype), MNRJ 26044–50, 26052–55 (paratypes).
- Brachycephalus brunneus*: state of PARANÁ: municipality of *Campina Grande do Sul*, Pico Paraná MHNCI 1919–20, Pico Caratua MNRJ 40289–91 (paratypes).
- Brachycephalus coloratus*: state of PARANÁ: municipality of *Piraquara*, Serra Baitaca, Estância Hidroclimática Recreio da Serra MNRJ 89949–50.
- Brachycephalus darkside*: state of MINAS GERAIS: municipality of *Ervália*, Parque Estadual da Serra do Brigadeiro, trilha do cruzeiro MNRJ 91327 (paratype).
- Brachycephalus didactylus*: state of RIO DE JANEIRO: municipality of *Paulo de Frontin*, Sacra Família do Tinguá MNRJ 4062–73 (paratypes), MNRJ 60136 (paratype).
- Brachycephalus ephippium*: state of MINAS GERAIS: municipality of *Fervedouro*, Serra do Pai Inácio MZUFV 2897. State of RIO DE JANEIRO: municipality of *Angra dos Reis* MNRJ 17458–59; municipality of *Cachoeira de Macacu*, Guapiaçu MNRJ 38104, 56517–18, 59946; municipality of *Itatiaia* AL-MN 667–68, 114, 2178, MNRJ 2155, 10789, 17455, 17456–57, 23281–86, 52427–44, MZUSP 9031, 104081, ZUEC 0008, 7149–54; municipality of *Mangaratiba* MNRJ 0578, 2542, 11574–83, 13264–272; municipality of *Nova Iguaçu*, Serra do Tinguá MNRJ 1495, 8157–69; municipality of *Paraty* MNRJ 0663, 2435, 10271; municipality of *Rio Claro*, Lídice MNRJ 25353–54, 66619–20, 71337; municipality of *Rio de Janeiro* MZUSP 103784–71 MNRJ 30920: *Pedra Branca* MNRJ 3327, 13818–19, 25408–09, 27577–78, 37579, MZUSP 34644, *Floresta da Tijuca* AL-MN 078–78^a, 0313–18, 3696–98, MNRJ 0640, 1870, 3959, 10205, 10215, 15332, 17431, 17453, 25346, 25368–71, 25412–14, 40781–99, 40801–04; MZUSP 76393, *Represa do Rio Grande* MZUSP 100277, 100281–318, 100366–766, ZUEC 971, *Floresta dos Macacos* MZUSP 100278–80; municipality of *Teresópolis* MNRJ 2764, 3311, 12471–72, 17438–39, 51580–83, ZUF RJ 3396, 3421, 3836–40, 3906, 3908, 3911–15, 4009, 4026, 4181, 4255–57, 4265–66, 4357–62, 4601–02, 4744–45, 5227–32, 6733: *Alto do Soberbo* MZUSP 49990–50056, *Comary* MNRJ 2091, 17436–37, 17452, *Parque Nacional da Serra dos Órgãos* MNRJ 17434–35, 17445, 17446, 17447–48, 17449, 17450, 17454, MZUSP 34646, 71707–08, 110205, ZUEC 8099–100, *Garrafão* MNRJ 71726–27, *Parque Estadual dos Três Picos*, *Vale da Revolta* MNRJ 50260–61, *Varginha* MNRJ 25377–84; municipality of *Valença*, Serra da Concórdia MNRJ 73395. State of SÃO PAULO: municipality of *Atibaia* MNRJ 25345, MZUSP 104203–04; municipality of *Bocaina* ZUF RJ 58–59; municipality of *Campinas*, *Observatório de Capricórnio* CFBH 0374, 0994–97, 1343, 2565–69, MNRJ 25347–52, ZUEC 5992, 6866, 6889, 9002, 9149–58; municipality of *Cotia* MHNCI 2611–16, MNRJ 18405–09, MZUSP 104149–58, ZUEC 1457–58, 1496–97; municipality of *Jundiaí*, Serra do Japí CFBH 2070–71, ZUEC 6852; municipality of *Mogi das Cruzes* MZUSP 104208–10, 136758, 136762–64, 136784, 137319, 138775, 138776; municipality of *Monteiro Lobato* MNRJ 70620–22; municipality of *Pindamonhangaba*, *Reserva Trabijú* MNRJ 70616–18, municipality of *Piquete* MZUSP 0534, 0810, 0851, 0864–66, 0871, 3820–46, 54387, municipality of *Santo André*, *Paranapiacaba* MNRJ 25367, MNRJ 42873, MZUSP 93350–51, ZUEC 445; municipality of *Santo Antônio do Pinhal* MNRJ 70628; municipality of *São José do Barreiro*, Serra da Bocaina, *Bonito* AL-MN 2261–2300, MNRJ 2143, 10783–86; municipality of *São José dos Campos*, *Distrito de São Francisco Xavier* MNRJ 70619, 70623–26, MZUSP 2761–62, Serra da Bocaina, *Fazenda Papagaio* MZUSP 104198–202, Serra da Bocaina, boundaries among the state of São Paulo and Rio de Janeiro AL-MN 894–899; municipality of *Taubaté*, *Reserva Pedra Branca* MNRJ 70627.
- Brachycephalus ferruginus*: state of PARANÁ: municipality of *Morretes*, Marumbi MHNCI 125, 128.
- Brachycephalus izecksohni*: state of PARANÁ: between the municipalities of *Guaratuba* and *Paranaguá*, Pico Torre de Prata CFBH 7381, 7382, 7384 (paratypes).
- Brachycephalus garbeanus*: state of RIO DE JANEIRO: municipality of *Nova Friburgo* MNRJ 17432, ZUF RJ 3408–10, 3414–15, Serra de Macaé MZUSP 0811 (lectotype), 1460–61 (paralectotypes), Macaé de Cima MNRJ 17440–41, MNRJ 25390–400, Morro São João MNRJ 17433, MNRJ 39615–18), *Alto da Caledônia* MNRJ 39583–614, MNRJ 67498), *Baixo Caledônia* MNRJ 57124, MNRJ 57293, *Teodoro Oliveira* MNRJ 51472–73, Serra Nevada MNRJ 39342–43.
- Brachycephalus hermogenesi*: state of SÃO PAULO: municipality of *Ubatuba* (MNRJ 18624, 18625, 18662–63 (paratypes)).
- Brachycephalus izecksohni*: state of PARANÁ: between the municipalities of *Guaratuba* and *Panaguá*, Pico Torre de Prata MNRJ 76259–60 (paratypes).
- Brachycephalus margaritatus*: state of RIO DE JANEIRO: municipality of *Engeiro Paulo Frontin*, Sacra Família do Tinguá MNRJ 39312 (holotype), MNRJ 21675, 25373–74, 25375–76, 25385, 25387–89, 25401, 39311, 39313–16 (paratypes); municipality of *Paty do Alferes* MNRJ 76100–01, ZUF RJ 2856; municipality of *Petrópolis* AL-MN 1367–68, MNRJ 60869–71, 62976–84, *Castelo Country Club* MNRJ 73700–702, *Castelo Montebello* MNRJ 70428–29, *Independência* AL-MN 1362–66, *Quitandinha* AL-MN 4141–42.
- Brachycephalus nodoterga*: state of SÃO PAULO: municipality of *Ilha Bela*, Morro do Ramalho MNRJ 23633–36, 23638–40; municipality of *São Paulo*, Serra da Cantareira MZUSP 0975 (holotype), 112785–91; municipality of *Salesópolis*, *Boracéia* MZUSP 30653, 30625–26, ZUEC 6073.
- Brachycephalus pernix*: state of PARANÁ: municipality of *Quatro Barras*, Serra da Baitaca, Morro Anhagava CFBH 2597–98 (paratypes), MHNCI 1818–19 (paratypes), 1820, 3000–04 (paratypes), MNRJ 17349 (holotype), ZUEC 9433–37 (para-

types).

Brachycephalus pitanga: state of SÃO PAULO: municipality of *São Luis do Paraitinga*, Núcleo de Santa Virginia MNRJ 60790–93 (paratypes).

Brachycephalus pulex: State of BAHIA: municipality of *Camacan*, Serra Bonita, CFBH 39373–39387, MNRJ 69646 (holotype).

Brachycephalus sulfuratus: State of PARANÁ: municipality of São José dos Pinhais, APA de Guaratuba ZUEC 16602; municipality of *Matinhos*, Parque Nacional Saint Hilaire/ Lange, Salto do Tigre MNRJ 86411. State of SANTA CATARINA: municipality of *São Francisco do Sul*, Centro de Estudos e Pesquisas Ambientais da Univille, Vila da Glória, Distrito do Saí CFBH 39137 (holotype), CFBH 39140 (paratype), CFBH 39329–30 (paratypes), 39332 (paratype). State of SÃO PAULO: municipality of Cananéia, Ilha do Cardoso MZUSP 129855.

Brachycephalus toby: State of SÃO PAULO: municipality of *Ubatuba*: praia dura, Morro do Corcovado MNRJ 76382–83 (paratypes).

Brachycephalus tridactylus: State of PARANÁ: municipality of *Guaraqueçaba*, Reserva Natural Salto Morato MNRJ 87908–10.

Brachycephalus vertebralis: state of RIO DE JANEIRO: municipality of *Paraty* MNRJ 11098 (holotype), 2022, 10515–18, 2053, 2338, 10599 paratype, 11095–96 paratypes, 11101–07, 11110–18, 11120–24, 11126–29, 11131–32 (paratypes).

APPENDIX II. List of voucher specimens included in molecular analysis, locality data, GenBank accession numbers, and references. In bold, sequences produced by the present work. Other sequences were obtained from GenBank. Abbreviations to Brazilian states: BA = Bahia, ES = Espírito Santo, PR = Paraná, RJ = Rio de Janeiro, SC = Santa Catarina, and SP = São Paulo.

Species	Collecting Data	Voucher	Genbank access number	Reference
<i>Brachycephalus actaeus</i>	Fazenda Morro Grande, São Francisco do Sul, SC	CFBH 39846	MG889451	Monteiro <i>et al.</i> (2018a)
<i>Brachycephalus actaeus</i>	Centro de Estudos e Pesquisas Ambientais da Univille, Vila da Glória, São Francisco do Sul, SC	CFBH 39848	MG889445	Monteiro <i>et al.</i> (2018a)
<i>Brachycephalus actaeus</i>	Serra da Palha, São Francisco do Sul, SC	CFBH 39850	MG889452	Monteiro <i>et al.</i> (2018a)
<i>Brachycephalus actaeus</i>	Estrada do Saí, São Francisco do Sul, SC	CFBH 39853	MG889450	Monteiro <i>et al.</i> (2018a)
<i>Brachycephalus alipioi</i>	Brazil: municipality of Vargem Alta, ES	CFBH 3566	HQ435690	Clemente-Carvalho <i>et al.</i> (2011)
<i>Brachycephalus albolineatus</i>	Morro Boa Vista, Jaraguá do Sul, SC	CFBH 41754	MG889434	Monteiro <i>et al.</i> (2018a)
<i>Brachycephalus auroguttatus</i>	not given	not given	KX025367	Firkowski <i>et al.</i> (2016)
	not given	not given	KX025366	Firkowski <i>et al.</i> (2016)
	not given	not given	KX025364	Firkowski <i>et al.</i> (2016)
	not given	not given	KX025365	Firkowski <i>et al.</i> (2016)
<i>Brachycephalus boticario</i>	not given	not given	KX025374	Firkowski <i>et al.</i> (2016)
	not given	not given	KX025373	Firkowski <i>et al.</i> (2016)
	not given	not given	KX025372	Firkowski <i>et al.</i> (2016)
	not given	not given	KX025371	Firkowski <i>et al.</i> (2016)
	not given	not given	KX025370	Firkowski <i>et al.</i> (2016)
<i>Brachycephalus brunneus</i>	not given	not given	KX025290	Firkowski <i>et al.</i> (2016)
	not given	not given	KX025289	Firkowski <i>et al.</i> (2016)
	not given	not given	KX025287	Firkowski <i>et al.</i> (2016)
	not given	not given	KX025288	Firkowski <i>et al.</i> (2016)

...Continued on the next page

APPENDIX II. (continued)

Species	Collecting Data	Voucher	Genbank access number	Reference
<i>Brachycephalus curupira</i>	Morro do Canal, Piraquara, PR	not given	KX025270	Firkowski <i>et al.</i> (2016)
	Morro do Canal, Piraquara, PR	not given	KX025272	Firkowski <i>et al.</i> (2016)
<i>Brachycephalus didactylus</i>	Brazil: Vale da Revolta (municipality of Teresópolis), RJ	CFBHt 11506	JX267467	Canedo & Haddad (2012)
<i>Brachycephalus ephippium</i>	Brazil: São Francisco Xavier (municipality of São José dos Campos), SP	CFBH 16828	HM216369	Clemente-Carvalho <i>et al.</i> (2011)
	Brazil: São Francisco Xavier (municipality of São José dos Campos), SP	not given	KP999209	Clemente-Carvalho <i>et al.</i> (2015)
	Brazil: Serra do Japi (municipality of Jundiá), SP	CFBH 16854	HM216361	Clemente-Carvalho <i>et al.</i> (2011)
	Brazil: municipality of Atibaia, SP	CFBH 16809	HM208306	Clemente-Carvalho <i>et al.</i> (2011)
<i>Brachycephalus ferruginus</i>	not given	not given	KX025238	Firkowski <i>et al.</i> (2016)
	not given	not given	KX025237	Firkowski <i>et al.</i> (2016)
	not given	not given	KX025236	Firkowski <i>et al.</i> (2016)
<i>Brachycephalus fuscolineatus</i>	not given	not given	KX025341	Firkowski <i>et al.</i> (2016)
	not given	not given	KX025340	Firkowski <i>et al.</i> (2016)
	not given	not given	KX025297	Firkowski <i>et al.</i> (2016)
	not given	not given	KX025339	Firkowski <i>et al.</i> (2016)
	Brazil: Macaé de Cima (municipality of Nova Friburgo), RJ	CFBH 16800	HQ435694	Clemente-Carvalho <i>et al.</i> (2011)
<i>Brachycephalus hermogenesi</i>	Brazil: municipality of Ubatuba, SP	CFBH29794	KU321531	Condez <i>et al.</i> (2016)
<i>Brachycephalus izecksohni</i>	not given	not given	KX025261	Firkowski <i>et al.</i> (2016)
	not given	not given	KX025260	Firkowski <i>et al.</i> (2016)
	not given	not given	KX025259	Firkowski <i>et al.</i> (2016)
	not given	not given	KX025258	Firkowski <i>et al.</i> (2016)
	not given	not given	KX025256	Firkowski <i>et al.</i> (2016)
<i>Brachycephalus leopardus</i>	not given	not given	KX025245	Firkowski <i>et al.</i> (2016)
	not given	not given	KX025244	Firkowski <i>et al.</i> (2016)
	not given	not given	KX025242	Firkowski <i>et al.</i> (2016)
	not given	not given	KX025243	Firkowski <i>et al.</i> (2016)
	not given	not given	KX025246	Firkowski <i>et al.</i> (2016)
<i>Brachycephalus mariaeterezae</i>	not given	not given	KX025350	Firkowski <i>et al.</i> (2016)
	not given	not given	KX025349	Firkowski <i>et al.</i> (2016)
	not given	not given	KX025347	Firkowski <i>et al.</i> (2016)
	not given	not given	KX025348	Firkowski <i>et al.</i> (2016)
	not given	not given	KX025346	Firkowski <i>et al.</i> (2016)

...Continued on the next page

APPENDIX II. (continued)

Species	Collecting Data	Voucher	Genbank access number	Reference
<i>Brachycephalus nodoterga</i>	not given	IB6317	KJ649788	Clemente-Carvalho <i>et al.</i> (2015)
	not given	IB6316	KJ649787	Clemente-Carvalho <i>et al.</i> (2015)
	not given	IB6315	KJ649786	Clemente-Carvalho <i>et al.</i> (2015)
	not given	IB6314	KJ649785	Clemente-Carvalho <i>et al.</i> (2015)
	not given	IB6313	KJ649784	Clemente-Carvalho <i>et al.</i> (2015)
	not given	IB6310	KJ649782	Clemente-Carvalho <i>et al.</i> (2015)
<i>Brachycephalus olivaceus</i>	not given	not given	KX025303	Firkowski <i>et al.</i> (2016)
	not given	not given	KX025302	Firkowski <i>et al.</i> (2016)
	not given	not given	KX025301	Firkowski <i>et al.</i> (2016)
<i>Brachycephalus bufonoides</i>	Serra Queimada trail, APA de Macaé de Cima, Lumiar, municipality of Nova Friburgo, RJ	ZUF RJ 15424	MH259790	Present work
	Serra Queimada trail, APA de Macaé de Cima, Lumiar, municipality of Nova Friburgo, RJ	ZUF RJ 15425	MH259789	Present work
	Serra Queimada trail, APA de Macaé de Cima, Lumiar, municipality of Nova Friburgo, RJ	ZUF RJ 15426	MH259791	Present work
	Serra Queimada trail, APA de Macaé de Cima, Lumiar, municipality of Nova Friburgo, RJ	ZUF RJ 15428	MH259788	Present work
	Serra Queimada trail, APA de Macaé de Cima, Lumiar, municipality of Nova Friburgo, RJ	ZUF RJ 15429	MH259792	Present work
<i>Brachycephalus pernix</i>	not given	not given	KX025222	Firkowski <i>et al.</i> (2016)
	not given	not given	KX025220	Firkowski <i>et al.</i> (2016)
	not given	not given	KX025221	Firkowski <i>et al.</i> (2016)
	not given	not given	KX025219	Firkowski <i>et al.</i> (2016)
	not given	not given	KX025218	Firkowski <i>et al.</i> (2016)
<i>Brachycephalus pitanga</i>	Brazil: municipality of São Luis do Paraitinga, SP	CFBH 16746	HQ435699	Clemente-Carvalho <i>et al.</i> (2011)
<i>Brachycephalus pombali</i>	not given	not given	KX025314	Firkowski <i>et al.</i> (2016)
	not given	not given	KX025310	Firkowski <i>et al.</i> (2016)
<i>Brachycephalus quiririensis</i>	not given	not given	KX025320	Firkowski <i>et al.</i> (2016)
	not given	not given	KX025319	Firkowski <i>et al.</i> (2016)
	not given	not given	KX025317	Firkowski <i>et al.</i> (2016)

...Continued on the next page

APPENDIX II. (continued)

Species	Collecting Data	Voucher	Genbank access number	Reference
<i>Brachycephalus sulfuratus</i>	Brazil: municipality of Cananeia, SP	CFBH39149	KU321535	Condez <i>et al.</i> (2016)
	Brazil: municipality of Quatro Barras, PR	CFBH39150	KU321534	Condez <i>et al.</i> (2016)
	Brazil: municipality of São Francisco do Sul, SC	CFBH39141	KU321532	Condez <i>et al.</i> (2016)
<i>Brachycephalus toby</i>	Brazil: municipality of Ubatuba, SP	CFBH 23002	HQ435701	Clemente-Carvalho <i>et al.</i> (2011)
<i>Brachycephalus tridactylus</i>	not given	not given	KX025391	Firkowski <i>et al.</i> (2016)
	not given	not given	KX025390	Firkowski <i>et al.</i> (2016)
	not given	not given	KX025388	Firkowski <i>et al.</i> (2016)
	not given	not given	KX025387	Firkowski <i>et al.</i> (2016)
	not given	not given	KX025389	Firkowski <i>et al.</i> (2016)
	Reserva Particular Salto Morato, Guaraqueçaba, PR	not given	MG889431	Monteiro <i>et al.</i> (2018a)
	Reserva Particular Salto Morato, Guaraqueçaba, PR	not given	MG889432	Monteiro <i>et al.</i> (2018a)
<i>Brachycephalus verrucosus</i>	Reserva Particular Salto Morato, Guaraqueçaba, PR	not given	MG889433	Monteiro <i>et al.</i> (2018a)
	not given	not given	KX025234	Firkowski <i>et al.</i> (2016)
<i>Brachycephalus vertebralis</i>	not given	not given	KX025323	Firkowski <i>et al.</i> (2016)
	Brazil: municipality of Ubatuba, SP	CFBH 7907	HQ435702	Clemente-Carvalho <i>et al.</i> (2011)
<i>Ischnocnema parva</i>	Brazil: municipality of Teresópolis, RJ	MNRJ43259	KC569991	Brusquetti <i>et al.</i> (2013)